Minimum BER Linear MIMO Transceivers With Adaptive Number of Substreams

Luis G. Ordóñez, *Student Member, IEEE*, Daniel P. Palomar, *Senior Member, IEEE*, Alba Pagès-Zamora, *Member, IEEE*, and Javier Rodríguez Fonollosa, *Senior Member, IEEE*

***Abstract*—MIMO systems with perfect channel state information at both sides of the link can adapt to the instantaneous channel conditions to optimize the spectral efficiency and/or the reliability of the communication. A low-complexity approach is the use of linear MIMO transceivers which are composed of a linear precoder at the transmitter and a linear equalizer at the receiver. The design of linear transceivers has been extensively studied in the literature with a variety of cost functions. In this paper, we focus on the minimum BER design, and show that the common practice of fixing *a priori* the number of data symbols to be transmitted per channel use inherently limits the diversity gain of the system. By introducing the number of symbols in the optimization process, we propose a minimum BER linear precoding scheme that achieves the full diversity of the MIMO channel. For the cases of uncorrelated/semicorrelated Rayleigh and uncorrelated Rician fading, the average BER performance of both schemes is analytically analyzed and characterized in terms of two key parameters: the array gain and the diversity gain.**

***Index Terms*—Analytical performance, linear MIMO transceiver, minimum BER design, ordered eigenvalues, Wishart matrices.**

I. Introduction

Wireless multiple-input multiple-output (MIMO) systems [1]–[3] have been attracting a great interest since they provide significant improvements in terms of spectral efficiency and reliability with respect to single-input single-output (SISO) systems. In order to simplify the study of MIMO systems, it is customary to divide them into an uncoded part, which transmits symbols drawn from some signal constellation, and a coded part that builds upon the uncoded system. Although the ultimate system performance depends on the combination of both parts, it is convenient to consider the uncoded and coded parts independently to simplify the design and analysis. This paper focuses on the uncoded part of the system and, specifically, on the employment of linear transceivers (composed of a linear precoder at the transmitter and a linear equalizer at the receiver).

The design of linear transceivers when perfect channel state information (CSI) is available at both sides of the link has been extensively studied in the literature according to a variety of criteria based on performance measures such as the signal-to-noise ratio (SNR), the mean square error (MSE), or the bit error rate (BER). The most common approach in the linear transceiver design literature is to adapt only the linear precoder/power allocation among the different substreams, assuming that the number of substreams κ and the corresponding constellations are fixed beforehand, e.g., [4]–[14]. For most of the reasonable criteria, the optimum linear transmitter diagonalizes the channel (possibly after a rotation of the data symbols) and establishes κ parallel substreams through the κ strongest channel eigenmodes [13], [14]. The available transmit power is then distributed among these substreams according to the specific design criterion and the instantaneous channel conditions.

In this paper, we show analytically for the cases of uncorrelated Rayleigh, semicorrelated Rayleigh, and uncorrelated Rician fading that the diversity gain of these schemes with κ substreams is at most given by $(n_\mathsf{T}-\kappa+1)(n_\mathsf{R}-\kappa+1)$, where n_T is the number of transmit and n_R the number of receive antennas. This diversity order can be far from the inherent diversity provided by the MIMO channel $n_\mathsf{T}n_\mathsf{R}$ [15]. To overcome this limitation, we then consider the introduction of the number of active substreams in the design criterion by fixing the global rate but allowing the use of an adaptive symbol constellation to compensate for the change in the number of transmitted symbols. Observe that this alternative restriction does not render ineffective the schemes available in the literature but simply implies an additional optimization stage on top of the classical design. Analytical diversity analysis confirms the intuitive notion that the full diversity $n_\mathsf{T}n_\mathsf{R}$ demands this final optimization step that has been commonly neglected in the literature. An exception is [16], where in the context of limited feedback linear precoding a similar adaptation of the number of substreams under a fixed rate constraint was proposed.

More specifically, this paper focuses on the minimum BER linear MIMO transceiver design. We first present the conventional design, in which the linear transmitter and receiver are designed to minimize the BER under a transmit power constraint and assuming that the number of transmitted symbols and constellations are fixed. This scheme is hereafter denoted

Manuscript received January 05, 2009; accepted January 05, 2009. First published February 24, 2009; current version published May 15, 2009. The associate editor coordinating the review of this paper and approving it for publication was Dr. Zhi Tian. This work was supported in part by the European Commission (27187 SURFACE), by the Spanish Ministry of Science and Innovation CONSOLIDER-INGENIO 2010 (CSD2008-00010 COMONSENS), by FEDER funds (TEC2006-06481), by the Catalan Government (2005SGR-00639), and by a RGC 618008 research grant. A portion this work was presented at the 2007 International Conference on Acoustics, Speech and Signal Processing (ICASSP), Honolulu, HI, April 2007.

L. G. Ordóñez, A. Pagès-Zamora, and J. Rodríguez Fonollosa are with the Department of Signal Theory and Communications, Technical University of Catalonia (UPC), 08034 Barcelona, Spain (e-mail: luisg@gps.tsc.upc.es; alba@gps.tsc.upc.es; fono@gps.tsc.upc.es).

D. P. Palomar is with the Department of Electronic and Computer Engineering, Hong Kong University of Science and Technology, Clear Water Bay, Kowloon, Hong Kong (e-mail: palomar@ust.hk).

Color versions of one or more of the figures in this paper are available online at http://ieeexplore.ieee.org.

Digital Object Identifier 10.1109/TSP.2009.2016253

as minBER-fixed design and was derived independently in [13] and [11]. Suboptimal results, in which the linear transmitter and receiver are designed under the same constraints but forced to diagonalize the channel can be found in [10], [12]. The substream optimization stage is considered next, i.e., the linear MIMO transceiver design with adaptive number of substreams (minBER-adap). Although the symbol constellation is jointly adapted with the number of substreams to keep the total transmission rate fixed, the design problem addressed here is substantially different from the classical problem formulation in the adaptive modulation literature [17]–[20], where, typically, the transmission rate is maximized under power and quality-of-service (QoS) constraints or the transmission power is minimized under QoS and rate constraints. For instance, in the context of MIMO linear transceivers, the design of both the constellations and the linear transceiver to minimize the transmit power under a QoS constraint (given in terms of BER) is addressed in [21].

The average BER performance of linear MIMO transceivers depends on the statistics of the eigenvalues associated with the channel eigenmodes user for communication [22]. Specifically, under the uncorrelated/semicorrelated Rayleigh or the uncorrelated Rician fading models, the performance of MIMO systems is strongly connected to Wishart distributed matrices, which can be jointly analyzed following the procedure in [23]. Indeed, based on the unifying framework proposed in [23], we complete these results and derive for the different Wishart distributions associated with the previous channel models:

(i) the cdf of the maximum weighted eigenvalue (out of a subset of the κ largest ones) (Theorem 3.1);
(ii) the first-order Taylor expansion of the marginal cdf of the k^{th} largest eigenvalue (Theorem 3.2); and
(iii) the first-order Taylor expansion of the cdf obtained in (i) (Theorem 3.3).

These results are then effectively applied to:

(a) bound the average BER performance of the minBER-fixed scheme (Theorem 4.1) and of the minBER-adap scheme (Theorem 5.2), and to
(b) characterize the high-SNR average BER performance of the minBER-fixed scheme (Theorem 4.2) and of the minBER-adap scheme (Theorem 5.3) in terms of diversity and array gain

under the previous channel models.

The rest of the paper is organized as follows. Section II is devoted to introducing the signal model and presenting the average BER performance measure. In Section III we define the channel model and derive the required results on the Wishart distribution ordered eigenvalues, which are later applied in the performance analysis. The design and performance analysis of the minimum BER linear transceiver with fixed and adaptive constellations is addressed in Sections IV and V, respectively. Finally, we summarize the main contribution of the paper in the last section.

II. System Design Problem and Performance Evaluation

In this section we present the general signal model corresponding to linear MIMO transceivers and formulate the minimum BER design problem. Additionally, we provide the procedure followed to analyze the performance of these schemes in fading channels.

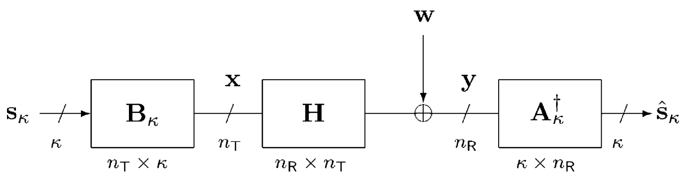

Fig. 1. Linear MIMO transceivers system model.

A. System Model

The signal model corresponding to a transmission through a general MIMO channel with n_T transmit and n_R receive antennas is

$$\mathbf{y} = \mathbf{H}\mathbf{x} + \mathbf{w} \tag{1}$$

where $\mathbf{x} \in \mathbb{C}^{n_\mathsf{T}}$ is the transmitted vector, $\mathbf{H} \in \mathbb{C}^{n_\mathsf{R} \times n_\mathsf{T}}$ is the channel matrix, $\mathbf{y} \in \mathbb{C}^{n_\mathsf{R}}$ is the received vector, and $\mathbf{w} \in \mathbb{C}^{n_\mathsf{R}}$ is a spatially white zero-mean circularly symmetric complex Gaussian noise vector normalized so that $\mathrm{E}\{\mathbf{w}\mathbf{w}^\dagger\} = \mathbf{I}_{n_\mathsf{R}}$.

Suppose that the MIMO communication system is equipped with a linear transceiver (see Fig. 1), then the transmitted vector containing the κ data symbols is given by

$$\mathbf{x} = \mathbf{B}_\kappa \mathbf{s}_\kappa \tag{2}$$

where $\mathbf{B}_\kappa \in \mathbb{C}^{n_\mathsf{T} \times \kappa}$ is the transmit matrix (linear precoder) and the data vector $\mathbf{s}_\kappa \in \mathbb{C}^{\kappa \times 1}$ gathers the $\kappa \leq \min\{n_\mathsf{T}, n_\mathsf{R}\}$ data symbols to be transmitted (zero-mean, unit-energy, and uncorrelated, i.e., $\mathrm{E}\{\mathbf{s}_\kappa \mathbf{s}_\kappa^\dagger\} = \mathbf{I}_\kappa$). We consider a fixed-rate data transmission and, hence, each data symbol $s_{k,\kappa}$ is drawn from an $M_{k,\kappa}$-dimensional constellation such that the total transmission rate

$$\mathsf{R} = \sum_{k=1}^{\kappa} \log_2 M_{k,\kappa} \tag{3}$$

is fixed for all channel realizations. The transmitted power is constrained such that

$$\mathbb{E}\left\{\|\mathbf{x}\|^2\right\} = \mathrm{tr}\{\mathbf{B}_\kappa \mathbf{B}_\kappa^\dagger\} \leq \mathsf{snr} \tag{4}$$

where snr denotes the average SNR per receive antenna. The estimated data vector at the receiver is

$$\hat{\mathbf{s}}_\kappa = \mathbf{A}_\kappa^\dagger \mathbf{y} = \mathbf{A}_\kappa^\dagger \left(\mathbf{H}\mathbf{B}_\kappa \mathbf{s}_\kappa + \mathbf{w}\right) \tag{5}$$

where $\mathbf{A}_\kappa^\dagger \in \mathbb{C}^{\kappa \times n_\mathsf{R}}$ is the receive matrix (linear equalizer). Observe from (5) that κ data streams are established for communication over the MIMO channel, where the k^{th} column of $\mathbf{B}_\kappa$ and $\mathbf{A}_\kappa$, denoted by $\mathbf{b}_{k,\kappa}$ and $\mathbf{a}_{k,\kappa}$, respectively, can be interpreted as the transmit and receive beam vectors associated with the k^{th} data stream or symbol $s_{k,\kappa}$

$$\hat{s}_{k,\kappa} = \mathbf{a}_{k,\kappa}^\dagger (\mathbf{H}\mathbf{b}_{k,\kappa} s_{k,\kappa} + \mathbf{n}_{k,\kappa}) \quad \text{for } k = 1, \ldots, \kappa \tag{6}$$

where $\mathbf{n}_{k,\kappa} = \sum_{i=1, i\neq k}^{\kappa} \mathbf{H}\mathbf{b}_{i,\kappa} s_{i,\kappa} + \mathbf{w}$ is the interference-plus-noise seen at the k^{th} substream.

B. Problem Statement

The linear MIMO transceiver design, i.e., the joint design of the receive and transmit matrices $(\mathbf{A}_\kappa, \mathbf{B}_\kappa)$ when perfect CSI is available at both sides of the link has been extensively studied since the 1970s under different measures of performance based on the MSEs, the SNRs, and the BERs [4]–[13]. A general unifying framework that embraces most of these design criteria has been proposed in [13] (see an up-to-date overview in [14]).

In this paper, we take the BER averaged over the κ data symbols as the performance measure:

$$\mathsf{BER}_\kappa\left(\{\rho_{k,\kappa}\}_{k=1}^{\kappa}\right) = \frac{1}{\kappa}\sum_{k=1}^{\kappa}\mathsf{BER}_{k,\kappa}(\rho_{k,\kappa}) \tag{7}$$

where $\rho_{k,\kappa}$ is the instantaneous SNR of the k^{th} substream in (6) given by

$$\rho_{k,\kappa} = \frac{|\mathbf{a}_{k,\kappa}^\dagger \mathbf{H}\mathbf{b}_{k,\kappa}|^2}{\mathbf{a}_{k,\kappa}^\dagger \mathbf{R}_{n_{k,\kappa}}\mathbf{a}_{k,\kappa}} \quad \text{for } k = 1,\ldots,\kappa \tag{8}$$

where $\mathbf{R}_{n_{k,\kappa}} = \sum_{i=1,i\neq k}^{\kappa}\mathbf{H}\mathbf{b}_{i,\kappa}\mathbf{b}_{i,\kappa}^\dagger\mathbf{H}^\dagger + \mathbf{I}_{N_\mathsf{R}}$ is the interference-plus-noise covariance matrix and $\mathsf{BER}_{k,\kappa}(\rho_{k,\kappa})$ is the corresponding instantaneous BER. In the presence of additive white Gaussian noise and assuming a Gray coding mapping, $\mathsf{BER}_{k,\kappa}(\rho_{k,\kappa})$ can be approximated[1] as [26, eq. (8.7)]

$$\mathsf{BER}_{k,\kappa}(\rho_{k,\kappa}) \approx \frac{\alpha_{k,\kappa}}{\log_2 M_{k,\kappa}}\mathcal{Q}\left(\sqrt{\beta_{k,\kappa}\rho_{k,\kappa}}\right) \quad \text{for } k = 1,\ldots,\kappa \tag{9}$$

where $\mathcal{Q}(\cdot)$ is the Gaussian $\mathcal{Q}$-function defined as [26, eq. (4.1)],

$$\mathcal{Q}(x) = \frac{1}{\sqrt{2\pi}}\int_x^\infty e^{-t^2/2}dt \tag{10}$$

and the parameters $\alpha_{k,\kappa}$ and $\beta_{k,\kappa}$ depend on the $M_{k,\kappa}$-dimensional modulation used to map the source bits to symbols (see the expressions for the most common digital modulation formats in [26, Sec. 8.1]).

To summarize, the problem studied in this paper is

$$\begin{array}{ll}\text{minimize} & \mathsf{BER}_\kappa\left(\{\rho_{k,\kappa}\}_{k=1}^{\kappa}\right)\\ \text{subject to} & \operatorname{tr}\left(\mathbf{B}_\kappa\mathbf{B}_\kappa\right) \le \mathsf{snr}\end{array} \tag{11}$$

in the following two cases:

(i) (minBER-fixed) fixed constellations (for some given rate R) and given κ, and optimization variables $(\mathbf{A}_\kappa, \mathbf{B}_\kappa)$.

(ii) (minBER-adap) fixed rate with optimization variables $(\kappa, \mathbf{A}_\kappa, \mathbf{B}_\kappa)$.

C. Performance Evaluation

For fading channels, the instantaneous BER defined in (7) does not offer representative information about the overall system performance and all different realizations of the random channel have to be taken into account, leading to the concept of average BER

$$\overline{\mathsf{BER}}_\kappa(\mathsf{snr}) \triangleq \mathbb{E}\left\{\mathsf{BER}_\kappa\left(\{\rho_{k,\kappa}\}_{k=1}^{\kappa}\right)\right\}. \tag{12}$$

[1]The given BER approximation is very tight in the BER region of practical interest ($\mathsf{BER} \ll 10^{-1}$). See the exact expression for QAM and PSK modulations in [24] and [25], respectively.

Given the limited availability of closed-form expressions for the average BER in (12), a convenient method to find simple performance measures is to allow a certain degree of approximation. In this respect, the most common approach is to shift the focus from exact performance to large SNR performance as done in [27], where the average BER versus SNR curve is characterized in terms of two key parameters: the diversity gain and the coding gain (also known as the array gain in the context of multiantenna systems [15]). The diversity gain represents the slope of the BER curve at high SNR and the coding gain (or array gain) determines the horizontal shift of the BER curve. Interestingly, both parameters only depend on the channel statistics through the first-order expansion of the pdf of the channel parameter [27].

In this paper, we analyze the average BER performance of both the minBER-fixed and the minBER-adap linear transceivers. More exactly, we find upper and lower bounds on the performance in uncorrelated/semicorrelated Rayleigh and uncorrelated Rician fading MIMO channels, with special emphasis on the high-SNR regime.

III. MIMO Channel Model and Probabilistic Characterization of Its Ordered Eigenvalues

When analyzing the performance of a communication system over a MIMO flat-fading channel, it is necessary to assume a certain channel fading distribution in order to obtain the average BER measure introduced in Section II-C. In this section, we first define the channel models used in the analytical performance analysis of the following sections and, then, we provide the required probabilistic characterization of the ordered eigenvalues of these channel models.

A. Rayleigh/Rician MIMO Channel Models

A MIMO channel with n_T transmit and n_R receive dimensions can be described by an $n_\mathsf{R} \times n_\mathsf{T}$ channel matrix $\mathbf{H}$, whose $(i,j)^{\text{th}}$ entry characterizes the propagation path between the j^{th} transmit and the i^{th} receive antenna. Usually, since there are a large number of scatters in the channel that contributes to the signal at the receiver, the application of the central limit theorem results in Gaussian distributed channel matrix coefficients. Analogously to the single antenna channel, this model is referred to as MIMO Rayleigh or Rician fading channel, depending whether the channel entries are zero-mean or not. More exactly, we assume that the channel matrix can be described as (see [23] and references therein)

$$\mathbf{H} = \sqrt{\frac{K_\mathsf{c}}{K_\mathsf{c}+1}}\overline{\mathbf{H}} + \sqrt{\frac{1}{K_\mathsf{c}+1}}\mathbf{\Sigma}_\mathsf{R}^{1/2}\mathbf{H}_\mathsf{w}\mathbf{\Sigma}_\mathsf{T}^{1/2} \tag{13}$$

where $K_\mathsf{c} \in [0,\infty)$ is power normalization factor known as the Rician K_c-factor, $\overline{\mathbf{H}}$ is a deterministic $n_\mathsf{R} \times n_\mathsf{T}$ matrix containing the line-of-sight components of the channel, $\mathbf{\Sigma}_\mathsf{T} = \left(\mathbf{\Sigma}_\mathsf{T}^{1/2}\right)\left(\mathbf{\Sigma}_\mathsf{T}^{1/2}\right)^\dagger$ is the transmit correlation matrix, $\mathbf{\Sigma}_\mathsf{R} = \left(\mathbf{\Sigma}_\mathsf{R}^{1/2}\right)\left(\mathbf{\Sigma}_\mathsf{R}^{1/2}\right)^\dagger$ is the receive correlation matrix, and $\mathbf{H}_\mathsf{w}$ is the random channel matrix with i.i.d. zero-mean unit-variance circulary symmetric Gaussian entries, i.e., $[\mathbf{H}_\mathsf{w}]_{ij} \sim \mathcal{CN}(0,1)$. For a fair comparison of the different cases, the total average received power is assumed to be constant and, hence, we can impose without loss of generality that $\operatorname{tr}(\boldsymbol{\Sigma}_{\mathsf{T}}) = n_{\mathsf{T}}$, $\operatorname{tr}(\boldsymbol{\Sigma}_{\mathsf{R}}) = n_{\mathsf{R}}$, and $\operatorname{tr}(\overline{\mathbf{H}}\overline{\mathbf{H}}^{\dagger}) = n_{\mathsf{R}} n_{\mathsf{T}}$. In this paper, we consider the following important particular cases of the general channel model in (13).

Definition 3.1: The uncorrelated Rayleigh MIMO fading channel model is defined as

$$\mathbf{H} = \mathbf{H}_{\mathsf{w}} \tag{14}$$

where $\mathbf{H}_{\mathsf{w}}$ is a $n_{\mathsf{R}} \times n_{\mathsf{T}}$ random channel matrix with i.i.d. zero-mean unit-variance complex Gaussian entries.

Definition 3.2: The semicorrelated Rayleigh fading MIMO channel model with correlation at the side with minimum number of antennas is defined as

$$\mathbf{H} = \begin{cases} \boldsymbol{\Sigma}^{1/2}\mathbf{H}_{\mathsf{w}} & n_{\mathsf{R}} \leq n_{\mathsf{T}} \\ \mathbf{H}_{\mathsf{w}}\boldsymbol{\Sigma}^{1/2} & n_{\mathsf{R}} > n_{\mathsf{T}} \end{cases} \tag{15}$$

where $\boldsymbol{\Sigma} = (\boldsymbol{\Sigma}^{1/2})(\boldsymbol{\Sigma}^{1/2})^{\dagger}$ is the $n \times n$ positive definite correlation matrix with $n = \min(n_{\mathsf{T}}, n_{\mathsf{R}})$ and $\mathbf{H}_{\mathsf{w}}$ is defined in (14).

Definition 3.3: The uncorrelated Rician fading MIMO channel model is defined as

$$\mathbf{H} = \sqrt{\frac{K_{\mathsf{c}}}{K_{\mathsf{c}}+1}}\overline{\mathbf{H}} + \sqrt{\frac{1}{K_{\mathsf{c}}+1}}\mathbf{H}_{\mathsf{w}} \tag{16}$$

where $K_{\mathsf{c}} \in (0, \infty)$, $\overline{\mathbf{H}}$ is a $n_{\mathsf{R}} \times n_{\mathsf{T}}$ deterministic matrix, and $\mathbf{H}_{\mathsf{w}}$ is defined in (14).

B. Ordered Eigenvalues of a General Class of Random Hermitian Matrices

Recently, the joint cdf and both the marginal cdf's and pdf's of the ordered eigenvalues of a general class of Hermitian random matrices have been derived in [23]. As formalized in Assumption 3.1, we concentrate on a more restrictive class[2] but general enough to include the channel models in Definitions 3.1–3.3.

Assumption 3.1: We consider the class of Hermitian random matrices, for which the joint pdf of its n nonzero ordered eigenvalues, $\lambda_1 \geq \cdots \geq \lambda_n \geq 0$, can be expressed as

$$\begin{aligned} f_{\boldsymbol{\lambda}}(\boldsymbol{\lambda}) &= f_{\boldsymbol{\lambda}}(\lambda_1, \ldots, \lambda_n) \\ &= K_{n,m}|\mathbf{E}(\boldsymbol{\lambda})||\mathbf{V}(\boldsymbol{\lambda})|\prod_{t=1}^{n}\varphi(\lambda_t) \end{aligned} \tag{17}$$

where $\mathbf{V}(\boldsymbol{\lambda})$ $(n \times n)$ is a Vandermonde matrix [29, eq. (6.1.32)] and matrix $\mathbf{E}(\boldsymbol{\lambda})$ $(n \times n)$ satisfies

$$[\mathbf{E}(\boldsymbol{\lambda})]_{u,v} = \zeta_u(\lambda_v) \quad \text{for } u, v = 1, \ldots, n. \tag{18}$$

The constant $K_{n,m}$ and the functions $\zeta_u(\lambda)$ and $\varphi(\lambda)$ depend on the distribution of the random matrix.

For the sake of completeness we now provide in Lemma 3.1 the expression of the marginal cdf of the k^{th} largest channel eigenvalue a random Hermitian matrix satisfying Assumption 3.1 and derive in Theorem 3.1 the cdf of the maximum weighted eigenvalue out of a subset of the κ largest ones. These results will prove useful in the analytical evaluation of the average performance of the minimum BER linear MIMO transceiver designs under analysis.

Lemma 3.1 ([23, Thm. 3.2])*:* The marginal cdf of the k^{th} $(1 \leq k \leq n)$ largest eigenvalue, λ_k, of a random Hermitian matrix satisfying Assumption 3.1 is given by

$$F_{\lambda_k}(\eta) = K_{n,m}\sum_{i=1}^{k}\sum_{\boldsymbol{\mu}\in\mathcal{P}(i)}|\mathbf{F}(\boldsymbol{\mu}, i; \eta)| \tag{19}$$

where $\mathcal{P}(i)$ is the set of all permutations $\boldsymbol{\mu} = (\mu_1, \ldots, \mu_n)$ of the integers $(1, \ldots, n)$ such that $(\mu_1 < \cdots < \mu_{i-1})$ and $(\mu_i < \cdots < \mu_n)$, matrix $\mathbf{F}(\boldsymbol{\mu}, i; \eta)$ $(n \times n)$ is defined as

$$[\mathbf{F}(\boldsymbol{\mu}, i; \eta)]_{u,v} = \begin{cases} \int_{\eta}^{\infty} \xi_{u,v}(\lambda)d\lambda & 1 \leq \mu_v < i \\ \int_{0}^{\eta} \xi_{u,v}(\lambda)d\lambda & i \leq \mu_v \leq n \end{cases} \tag{20}$$

for $u, v = 1, \ldots, n$ and the function $\xi_{u,v}(\lambda) = \zeta_u(\lambda)\varphi(\lambda)\lambda^{v-1}$ (see Assumption 3.1).

Theorem 3.1: Let us define the random variable $\lambda_{\mathcal{K}}$ as

$$\lambda_{\mathcal{K}} = \max_{k\in\mathcal{K}} \frac{\lambda_k}{\theta_k} \tag{21}$$

where λ_k is the k^{th} largest eigenvalue of a random Hermitian matrix satisfying Assumption 3.1, $\mathcal{K}$ is a nonempty subset of $\{1, \ldots, n\}$ of cardinality $1 < |\mathcal{K}| \leq n$, and $\{\theta_k\}_{k\in\mathcal{K}}$ are some given positive constants such that $(\theta_{\mathcal{K}_1} \geq \cdots \geq \theta_{\mathcal{K}_{|\mathcal{K}|}})$,[3] where $\mathcal{K}_i$ denotes the i^{th} element of $\mathcal{K}$ ordered in increasing order. Then, the cdf of $\lambda_{\mathcal{K}}$ is

$$F_{\lambda_{\mathcal{K}}}(\eta) = K_{n,m}\sum_{\boldsymbol{i}\in\mathcal{S}}\frac{1}{\tau(\boldsymbol{i})}\mathcal{T}\{\mathbf{T}(\boldsymbol{i}; \boldsymbol{\vartheta}(\eta))\} \tag{22}$$

where $\boldsymbol{\vartheta}(\eta) = (\vartheta_1(\eta), \ldots, \vartheta_n(\eta))$ with

$$\vartheta_k(\eta) = \vartheta_k \cdot \eta = \begin{cases} \theta_k\eta & k \in \mathcal{K} \\ \vartheta_{k-1}(\eta) & k \notin \mathcal{K},\ k > \mathcal{K}_1 \\ \infty & k \notin \mathcal{K},\ k < \mathcal{K}_1 \end{cases} \tag{23}$$

for $k = 1, \ldots, n$, the summation over $\boldsymbol{i} = (i_1, \ldots, i_n)$ is for all $\boldsymbol{i}$ in the set $\mathcal{S}$ defined as[4]

$$\begin{aligned} \mathcal{S} = \{\boldsymbol{i} \in \mathbb{N}^n \,|\, &\max(i_{s-1}, s) \leq i_s \leq n, \\ &i_s \neq r \text{ if } \vartheta_r(\eta) = \vartheta_{r+1}(\eta)\} \end{aligned} \tag{24}$$

and

$$\tau(\boldsymbol{i}) = \prod_{u=1}^{n}\left((1 - \delta_{i_u,i_{u+1}})\sum_{v=1}^{u}\delta_{i_u,i_v}\right)! \tag{25}$$

where $\delta_{u,v}$ denotes the Kronecker delta. The operator $\mathcal{T}\{\cdot\}$ is defined in Appendix A and the tensor $\mathbf{T}(\boldsymbol{i}; \boldsymbol{\vartheta}(\eta))$ $(n \times n \times n)$ is defined as

$$[\mathbf{T}(\boldsymbol{i}; \boldsymbol{\vartheta}(\eta))]_{u,v,t} = \int_{\vartheta_{i_t+1}(\eta)}^{\vartheta_{i_t}(\eta)} \xi_{u,v}(\lambda)d\lambda \tag{26}$$

[2]The ordered eigenvalues of the random matrices satisfying Assumption 3.1 were also recently analyzed in [28].

[3]Note that if $\{\theta_k\}_{k\in\mathcal{K}}$ are in increasing order, then $\lambda_{\mathcal{K}} = \lambda_1$.

[4]Note that $i_n = n$ and by definition $i_0 = 0$, $i_{n+1} = n + 1$ and $\vartheta_{n+1}(\eta) = 0$.

for $u,v,t = 1,\dots,n$, where $\xi_{u,v}(\lambda) = \zeta_u(\lambda)\varphi(\lambda)\lambda^{v-1}$ (see Assumption 3.1).

Proof: See Appendix B-I

When focusing on the high-SNR regime, the system performance does not depend anymore on the exact probabilistic characterization of the fading channel, but only on its behavior near the origin [27]. For this reason, we present in the following theorems the first-order Taylor expansion around zero of the cdf's given in Lemma 3.1 and Theorem 3.1.

Assumption 3.2: Let the Taylor expansion[5] of the function $\zeta_u(\lambda)\varphi(\lambda)$ (see Assumption 3.1) be

$$\zeta_u(\lambda)\varphi(\lambda) = \sum_{t=c(u)}^{\infty} \frac{a_u(t)}{t!}\lambda^t \tag{28}$$

where $a_u(t)$ is such that $a_u(t)=0$ for $t<c(u)$ and let matrix $\mathbf{M}$ $(n\times n)$, defined as

$$[\mathbf{M}]_{u,v} = \begin{cases} a_u(c+v) & 1\le v\le n-k+1 \\ b_{u,v} & n-k+1<v\le n \end{cases} \tag{29}$$

for $u = 1,\dots,n$, have nonzero determinant, where $c=\min_u c(u)$ and

$$b_{u,v} = \int_0^\infty \xi_{u,v}(\lambda)d\lambda = \int_0^\infty \zeta_u(\lambda)\varphi(\lambda)\lambda^{v-1}d\lambda. \tag{30}$$

Theorem 3.2: Under Assumption 3.2, the first-order Taylor expansions of the marginal cdf, $F_{\lambda_k}(\eta)$, and the marginal pdf, $f_{\lambda_k}(\eta)$, of the k^{th} largest eigenvalue of a random Hermitian matrix satisfying Assumption 3.1 are

$$F_{\lambda_k}(\eta) = \left(\frac{a_k}{d_k+1}\right)\eta^{d_k+1} + o\left(\eta^{d_k+1}\right) \tag{31}$$

$$f_{\lambda_k}(\eta) = a_k\eta^{d_k} + o\left(\eta^{d_k}\right) \tag{32}$$

with a_k and d_k defined as

$$a_k = K_{n,m}(d_k+1)\sum_{\boldsymbol{\nu}} \frac{1}{\tau(\boldsymbol{\nu})}|\mathbf{F}(\boldsymbol{\nu})| \tag{33}$$

$$d_k = (c-n-k-1)(n-k+1)-1 \tag{34}$$

[5]The Taylor expansion of a function $f(x)$ around a point x_0 is [30, eq. (25.2.24)],

$$f(x) = \sum_{t=0}^{\infty} \frac{f^{(t)}(x)|_{x=x_0}}{t!}(x-x_0)^t$$
$$= \sum_{t=0}^{r} \frac{f^{(t)}(x)|_{x=x_0}}{t!}(x-x_0)^t + o\left((x-x_0)^r\right) \tag{27}$$

where $f^{(t)}(x)$ denotes the t^{th} derivative of $f(x)$ and we say that $f(x) = o(g(x))$ if $f(x)/g(x)\to 0$ as $x\to 0$[31, eq. (1.3.1)].

where the summation over $\boldsymbol{\nu} = (\nu_1,\dots,\nu_{n-k+1})$ is for all permutations of the integers $(1,\dots,n-k+1)$, $\tau(\boldsymbol{\nu})$ is

$$\tau(\boldsymbol{\nu}) = \prod_{v=1}^{n-k+1}(c+v+\nu_v-1)! \tag{35}$$

and matrix $\mathbf{F}(\boldsymbol{\nu})$ $(n\times n)$ is defined as shown in (36) at the bottom of the page.

Proof: See Appendix B-II

Theorem 3.3: Under Assumption 3.2, the first-order Taylor expansions of the cdf, $F_{\lambda_{\mathcal{K}}}(\eta)$, and the pdf, $f_{\lambda_{\mathcal{K}}}(\eta)$, of the random variable $\lambda_{\mathcal{K}}$ introduced in Theorem 3.1 when[6] $\{1\}\subseteq\mathcal{K}\subseteq\{1,\dots,n\}$ are

$$F_{\lambda_{\mathcal{K}}}(\eta) = \left(\frac{a_{\mathcal{K}}}{d_{\mathcal{K}}+1}\right)\eta^{d_{\mathcal{K}}+1} + o\left(\eta^{d_{\mathcal{K}}+1}\right) \tag{37}$$

$$f_{\lambda_{\mathcal{K}}}(\eta) = a_{\mathcal{K}}\eta^{d_{\mathcal{K}}} + o\left(\eta^{d_{\mathcal{K}}}\right) \tag{38}$$

with $a_{\mathcal{K}}$ and $d_{\mathcal{K}}$ defined as

$$a_{\mathcal{K}} = K_{n,m}\sum_{\boldsymbol{i}\in\mathcal{S}} \frac{d_{\mathcal{K}}+1}{\tau(\boldsymbol{i})}\sum_{\boldsymbol{\nu}} \mathcal{T}\{\mathbf{T}(\boldsymbol{\nu},\boldsymbol{i};\boldsymbol{\vartheta})\} \tag{39}$$

$$d_{\mathcal{K}} = (c+n)n \tag{40}$$

where the summation over $\boldsymbol{i}\in\mathcal{S}$ and $\tau(\boldsymbol{i})$ are defined as in Theorem 3.1, the summation over $\boldsymbol{\nu} = (\nu_1,\dots,\nu_n)$ is for all permutations of integers $(1,\dots,n)$, the tensor $\mathbf{T}(\boldsymbol{\nu},\boldsymbol{i};\boldsymbol{\vartheta})$ $(n\times n\times n)$ is defined as

$$[\mathbf{T}(\boldsymbol{\nu},\boldsymbol{i};\boldsymbol{\vartheta})]_{u,v,t} = \frac{1}{c(\nu_v+v)c(v)!}a_u(c(v)) \left(\vartheta_{i_t}^{c(\nu_v+v)} - \vartheta_{i_t+1}^{c(\nu_v+v)}\right) \tag{41}$$

for $u,v,t = 1,\dots,n$, and $c(v) = c+v-1$.

Proof: See Appendix B-C.

C. Ordered Eigenvalues of Rayleigh/Rician Fading Channels

In this section we consider the different distributions of $\mathbf{HH}^\dagger$ or $\mathbf{H}^\dagger\mathbf{H}$ that result when $\mathbf{H}$ follows the MIMO channel models described in Definitions 3.1–3.3. For these cases, we provide the expressions for the parameters describing the general joint pdf of the eigenvalues in Assumption 3.1, as well as the expressions needed to particularize the results given in Section III-B. Defining the random Hermitian matrix $\mathbf{W}$ as

$$\mathbf{W} = \begin{cases} \mathbf{HH}^\dagger & n_{\mathsf{R}}\le n_{\mathsf{T}} \\ \mathbf{H}^\dagger\mathbf{H} & n_{\mathsf{R}}>n_{\mathsf{T}} \end{cases} \tag{42}$$

we can derive without loss of generality the statistical properties of the nonzero channel eigenvalues by analyzing the eigenvalues

[6]For simplicity of the proof we make the assumption that $\{1\}\subseteq\mathcal{K}$, although it is not really necessary.

$$[\mathbf{F}(\boldsymbol{\nu})]_{u,v} = \begin{cases} \frac{(c+v+\nu_v-2)!}{(c+\nu_v-1)!}a_u(c+\nu_v-1) & 1\le v\le n-k+1 \\ b_{u,v} & n-k+1<v\le n \end{cases} \quad \text{for } u,v=1,\dots,n. \tag{36}$$

TABLE I
PARAMETERS OF THE UNCORRELATED AND MIN-SEMICORRELATED RAYLEIGH FADING MIMO CHANNELS (DEFINITIONS 3.1 AND 3.2)

	$\mathbf{W} \sim \mathcal{W}_n(m, \mathbf{0}_n, \mathbf{I}_n)$	$\mathbf{W} \sim \mathcal{W}_n(m, \mathbf{0}_n, \mathbf{\Sigma})$
$K_{n,m}$	$\prod_{i=1}^{n} \frac{1}{(m-i)!(n-i)!}$	$\prod_{i=1}^{n} \frac{1}{\sigma_i^m (m-i)!} \prod_{i<j}^{n} \frac{\sigma_i \sigma_j}{\sigma_j - \sigma_i}$
$\varphi(\lambda)$	$e^{-\lambda}\lambda^{m-n}$	λ^{m-n}
$\zeta_u(\lambda)$	λ^{u-1}	$e^{-\lambda/\sigma_u}$
$\xi_{u,v}(\lambda)$	$e^{-\lambda}\lambda^{(c+u+v-2)}$	$e^{-\lambda/\sigma_u}\lambda^{(c+v-1)}$
$\int_\eta^\infty \xi_{u,v}(\lambda)d\lambda$	$\Gamma(c+u+v-1, \eta)$	$\sigma_u^{(c+v)}\Gamma(c+v, \eta/\sigma_u)$
$\int_0^\eta \xi_{u,v}(\lambda)d\lambda$	$\gamma(c+u+v-1, \eta)$	$\sigma_u^{(c+v)}\gamma(c+v), \eta/\sigma_u)$
$a_u(v)$	$\frac{v!}{(v-(c+u-1))!}(-1)^{(v-(c+u-1))}, \quad v \geq c+u-1$	$\frac{v!}{(v-c)!}(-\sigma_u)^{c-t}, \quad v \geq c$
$b_{u,v}$	$(c+u+v-2)!$	$\sigma_u^{(c+v)}(c+v-1)!$
c	$m-n$	$m-n$

of $\mathbf{W}$, since the nonzero eigenvalues of $\mathbf{H}\mathbf{H}^\dagger$ and $\mathbf{H}^\dagger\mathbf{H}$ coincide.

1) Uncorrelated Rayleigh Fading MIMO Channel: Given the MIMO channel $\mathbf{H}$ in Definition 3.1, the random Hermitian matrix $\mathbf{W}$ $(n \times n)$ in (47) follows a complex uncorrelated central Wishart distribution [32], denoted as $\mathbf{W} \sim \mathcal{W}_n(m, \mathbf{0}_n, \mathbf{I}_n)$, where $n = \min(n_\mathsf{T}, n_\mathsf{R})$ and $m = \max(n_\mathsf{T}, n_\mathsf{R})$. The joint pdf of the ordered eigenvalues of $\mathbf{W} \sim \mathcal{W}_n(m, \mathbf{0}_n, \mathbf{I}_n)$ satisfies Assumption 3.1 and the parameters to particularize the results in Lemma 3.1 and Theorem 3.1 are provided in Table I[7] (see [23, Sec. 4] for details). Finally, in order to apply Theorems 3.2 and 3.3, we just need to calculate

$$b_{u,v} = \int_0^\infty \xi_{u,v}(\lambda)d\lambda = (m-n+u+v-2)! \tag{43}$$

and the Taylor expansion of $\zeta_u(\lambda)\varphi(\lambda)$. Using the Taylor expansion of $e^{-\lambda}$ (see [30, eq. (4.2.1)]), it follows that

$$\zeta_u(\lambda)\varphi(\lambda) = \sum_{t=c(u)}^{\infty} \frac{1}{(t-c(u))!}(-1)^{t-c(u)}\lambda^t \tag{44}$$

where the function $c(u) = m-n+u-1$, $c = \min_u c(u) = m-n$.

2) Min-Semicorrelated Rayleigh Fading MIMO Channel: Given the MIMO channel $\mathbf{H}$ in Definition 3.2, the random Hermitian matrix $\mathbf{W}$ $(n \times n)$ in (47) follows a complex correlated central Wishart distribution [32], denoted as $\mathbf{W} \sim \mathcal{W}_n(m, \mathbf{0}_n, \mathbf{\Sigma})$, where $\mathbf{\Sigma}$ is the $n \times n$ positive definite correlation matrix with eigenvalues $\boldsymbol{\sigma} = (\sigma_1, \ldots, \sigma_n)$ ordered such that $(\sigma_1 > \cdots > \sigma_n > 0)$. The joint pdf of the ordered eigenvalues of $\mathbf{W} \sim \mathcal{W}_n(m, \mathbf{0}_n, \mathbf{\Sigma})$ satisfies Assumption 3.1 and the parameters to particularize the results in Lemma 3.1 and Theorem 3.1 are provided in Table I (see [23, Sec. 4] for details). Finally, in order to apply Theorems 3.2 and 3.3, we just need to calculate

$$b_{u,v} = \int_0^\infty \xi_{u,v}(\lambda)d\lambda = \sigma_u^{(m-n+v)}(m-n+v-1)! \tag{45}$$

and the Taylor expansion of $\zeta_u(\lambda)\varphi(\lambda)$. Using the Taylor expansion of the $e^{-\lambda}$ (see [30, eq. (4.2.1)]), it follows that

$$\zeta_u(\lambda)\varphi(\lambda) = \sum_{t=c}^{\infty} \frac{1}{(t-c)!}(-\sigma_u)^{c-t}\lambda^t \tag{46}$$

where $c = m-n$.

3) Uncorrelated Rician Fading MIMO Channel: Given the MIMO channel in Definition 3.3, the random Hermitian matrix $\widetilde{\mathbf{W}} = (K_\mathsf{c}+1)\mathbf{W}$, where $\mathbf{W}$ is given in (42), follows a complex uncorrelated noncentral Wishart distribution [32], denoted as $\widetilde{\mathbf{W}} \sim \mathcal{W}_n(m, \mathbf{\Omega}, \mathbf{I}_n)$, where the noncentrality parameter $\mathbf{\Omega}$ is defined as

$$\mathbf{\Omega} = \begin{cases} K_\mathsf{c}\overline{\mathbf{H}}\overline{\mathbf{H}}^\dagger & n_\mathsf{R} \leq n_\mathsf{T} \\ K_\mathsf{c}\overline{\mathbf{H}}^\dagger\overline{\mathbf{H}} & n_\mathsf{R} > n_\mathsf{T} \end{cases} \tag{47}$$

with eigenvalues $\boldsymbol{\omega} = (\omega_1, \ldots, \omega_n)$ ordered such that $(\omega_1 > \cdots > \omega_n > 0)$. Observe that in this case the nonzero channel eigenvalues, i.e., the eigenvalues of $\mathbf{W}$, are a scaled version of the eigenvalues of the complex uncorrelated central Wishart distributed matrix $\widetilde{\mathbf{W}}$. The joint pdf of the ordered eigenvalues of $\widetilde{\mathbf{W}} \sim \mathcal{W}_n(m, \mathbf{\Omega}, \mathbf{I}_n)$ satisfies Assumption 3.1 and the parameters to particularize the results in Lemma 3.1 and Theorem 3.1 are provided in Table II[8] (see [23, Sec. 4], for details). Finally, in order to particularize Assumption 3.2 and Theorems

[7]In Table I, $\gamma(\cdot,\cdot)$ denotes the lower incomplete gamma function [30, eq. (6.5.2)], and $\Gamma(\cdot,\cdot)$ denotes the upper incomplete gamma function [30, eq. (6.5.3)].

[8]In Table II, ${}_0F_1(\cdot;\cdot)$ and ${}_1F_1(\cdot;\cdot)$ are generalized hypergeometric functions [33, eq. (9.14.1)], and $Q_{\cdot,\cdot}(\cdot,\cdot)$ denotes the Nuttall Q function [26, eq. (4.104)], which is not considered to be a tabulated function. However, it can be easily calculated as shown in [34].

TABLE II
PARAMETERS OF THE UNCORRELATED RICIAN FADING MIMO CHANNEL (DEFINITION 3.3)

	$\widetilde{\mathbf{W}} \sim \mathcal{W}_n(m, \mathbf{\Omega}, \mathbf{I}_n)$
$K_{n,m}$	$\frac{e^{-\sum_{i=1}^{n}\omega_i}}{((m-n)!)^n}\prod_{i<j}^{n}\frac{1}{(\omega_j-\omega_i)}$
$\varphi(\lambda)$	$e^{-\lambda}\lambda^{m-n}$
$\zeta_u(\lambda)$	${}_0F_1(c+1;\omega_u\lambda)$
$\xi_{u,v}(\lambda)$	${}_0F_1(c+1;\omega_u\lambda)e^{-\lambda}\lambda^{c+v-1}$
$\int_0^{\eta}\xi_{u,v}(\lambda)d\lambda$	$(c+v-1)!{}_1F_1(c+v;c+1;\omega_u) - \frac{e^{\omega_u}2^{1-v}(c)!}{\left(\sqrt{2\omega_u}\right)^c}Q_{c+2v-1,c}\left(\sqrt{2\omega_u},\sqrt{2\eta}\right)$
$\int_{\eta}^{\infty}\xi_{u,v}(\lambda)d\lambda$	$\frac{e^{\omega_u}2^{1-v}c!}{\left(\sqrt{2\omega_u}\right)^c}Q_{c+2v-1,c}\left(\sqrt{2\omega_u},\sqrt{2\eta}\right)$
$a_u(v)$	$\sum_{i=0}^{t-c}\binom{t}{c+i}\frac{(c+i)!}{(n+i+1)!i!}\omega_u^i(-1)^{t-(c+i)}, \quad v \geq c$

3.2 and 3.3, we just need to calculate the Taylor expansion of $\zeta_u(\lambda)\varphi(\lambda) = \sum_{t=c}^{\infty} a_u(t)\lambda^t/t!$ and

$$b_{u,v} = \int_0^{\infty}\xi_{u,v}(\lambda)d\lambda = (m-n+v-1)! \, {}_1F_1(m-n+v;m-n+1;\omega_u). \quad (48)$$

Noting that [30, eq. (9.6.47)]

$${}_0F_1(n+1;\lambda) = n!\lambda^{-n/2}I_n(2\sqrt{\lambda}) \quad (49)$$

where $I_n(\cdot)$ is the modified Bessel function of the first kind of integer order n[30, eq. (9.6.10)]

$$I_n(\lambda) = \left(\frac{\lambda}{2}\right)^n \sum_{i=0}^{\infty}\frac{\left(\frac{\lambda^2}{4}\right)^i}{(n+i)!i!} \quad (50)$$

it follows that

$$\begin{aligned}\frac{d^t}{d\lambda^t}\left(\zeta_u(\lambda)\varphi(\lambda)\right) &= \frac{(m-n)!}{\left(\sqrt{\omega_u}\right)^{m-n}} \frac{d^t}{d\lambda^t}\left(e^{-\lambda}\lambda^{(m-n)/2}I_{m-n}(2\sqrt{\omega_u\lambda})\right) \quad (51)\\ &= (m-n)!\sum_{i=0}^{\infty}\frac{\omega_u^i}{(n+i)!i!}\frac{d^t}{d\lambda^t}\left(e^{-\lambda}\lambda^{c+i}\right) \quad (52)\end{aligned}$$

where $c = m-n$. Then, using Leibniz's Rule (see [30, eq. (3.3.8)]), we have that

$$\frac{d^t}{d\lambda^t}\left(e^{-\lambda}\lambda^{c+i}\right) = \sum_{r=0}^{t}\binom{t}{r}\frac{(c+i)!}{(c+i-r)!}(-1)^{t-r}e^{-\lambda}\lambda^{c+i-r} \quad (53)$$

and, using (51) and (53)

$$\begin{aligned}a_u(t) &= \left.\frac{d^t}{d\lambda^t}\left(\zeta_u(\lambda)\varphi(\lambda)\right)\right|_{\lambda=0}\\ &= \begin{cases}0 & t<c\\ \sum_{i=0}^{t-c}\binom{t}{c+i}\frac{(c+i)!}{(n+i+1)!i!}\omega_u^i(-1)^{t-(c+i)} & t \geq c\end{cases}. \quad (54)\end{aligned}$$

IV. MINBER LINEAR MIMO TRANSCEIVER WITH FIXED NUMBER OF SUBSTREAMS

Traditionally, the linear MIMO transceiver design has been addressed using analytically tractable cost functions based on the MSEs or the SNRs of the established substreams. Only recently, the system has been designed in [11] and [13] using the BER as performance measure, when equal constellations are used on all substreams. In this section we present this minimum BER linear transceiver and analyze its average BER performance for the Rayleigh and Rician MIMO channel models introduced in Definitions 3.1–3.3.

A. Linear Transceiver Design

Following the approach in [13], the optimum receive matrix $\mathbf{A}_\kappa$, for a given transmit matrix $\mathbf{B}_\kappa$, is the Wiener filter solution [13, eq. (7)]:

$$\mathbf{A}_\kappa = \left(\mathbf{H}\mathbf{B}_\kappa\mathbf{B}_\kappa^\dagger\mathbf{H}^\dagger + \mathbf{I}_{n_\mathsf{R}}\right)^{-1}\mathbf{H}\mathbf{B}_\kappa \quad (55)$$

independently of the design cost function. Specifically, under the minimum BER design criterion when equal constellations are used on all κ substreams, the transmit matrix $\mathbf{B}_\kappa$ is given by [13, Sec. V.C and eq. (15)]

$$\mathbf{B}_\kappa = \mathbf{U}_\kappa\sqrt{\mathbf{P}_\kappa}\mathbf{Q}_\kappa \quad (56)$$

where $\mathbf{U}_\kappa \in \mathbb{C}^{n_\mathsf{T}\times\kappa}$ has as columns the eigenvectors of $\mathbf{H}^\dagger\mathbf{H}$ corresponding to the κ largest nonzero eigenvalues $\lambda_1 \geq \cdots \geq \lambda_\kappa$, $\mathbf{Q}_\kappa \in \mathbb{C}^{\kappa\times\kappa}$ is a unitary matrix such that $\left(\mathbf{I}_\kappa + \mathbf{B}_\kappa^\dagger\mathbf{H}^\dagger\mathbf{H}\mathbf{B}_\kappa\right)^{-1}$ has identical diagonal elements (see

[13, Sec. IV.B], for details), and $\mathbf{P}_\kappa \in \mathbb{C}^{\kappa\times\kappa}$ is a diagonal matrix with diagonal entries equal to

$$p_{k,\kappa} = \left(\mu\lambda_k^{-1/2} - \lambda_k^{-1}\right)^+ \quad \text{for } k = 1,\dots,\kappa \tag{57}$$

where μ is chosen to satisfy the power constraint in (4) with equality, i.e.,

$$\sum_{k=1}^{\kappa} p_{k,\kappa} = \mathsf{snr}. \tag{58}$$

B. Analytical Performance

Given the optimum receive matrix in (55) and the optimum transmit matrix in (56), the communication process is diagonalized up to a specific rotation that forces all κ data symbols to have the same MSE

$$\mathsf{mse}_\kappa \triangleq \mathsf{mse}_{k,\kappa} = \frac{1}{\kappa}\sum_{i=1}^{\kappa}(1+p_{i,\kappa}\lambda_i)^{-1} \tag{59}$$

and, hence, the same instantaneous SNR

$$\begin{aligned}\rho_\kappa \triangleq \rho_{k,\kappa} &= \mathsf{mse}_\kappa^{-1} - 1\\ &= \left(\frac{1}{\kappa}\sum_{i=1}^{\kappa}\left(1+p_{i,\kappa}\lambda_i\right)^{-1}\right)^{-1} - 1.\end{aligned} \tag{60}$$

Thus, the minBER-fixed design transmits a rotated version of the κ data symbols through the κ strongest channel eigenmodes, so that all data symbols experience the same BER performance. The instantaneous BER averaged over the κ data symbols defined in (7) is then given by

$$\mathsf{BER}_\kappa(\mathsf{snr}) = \frac{\alpha_\kappa}{\log_2 M_\kappa}\mathcal{Q}\left(\sqrt{\beta_\kappa\rho_\kappa}\right) \tag{61}$$

where $M_\kappa \triangleq M_{k,\kappa}$, $\alpha_\kappa \triangleq \alpha_{k,\kappa}$, $\beta_K \triangleq \beta_{k,\kappa}$ for $k = 1,\dots,\kappa$, since all constellations are equal. Now, taking into account all possible channel states, the average BER is obtained as

$$\begin{aligned}\overline{\mathsf{BER}}_\kappa(\mathsf{snr}) &= \mathbb{E}\left\{\mathsf{BER}_\kappa(\mathsf{snr})\right\}\\ &= \frac{\alpha_\kappa}{\log_2 M_\kappa}\int_0^\infty \mathcal{Q}\left(\sqrt{\beta_\kappa\rho}\right) f_{\rho_\kappa}(\rho)d\rho\end{aligned} \tag{62}$$

where $f_{\rho_\kappa}(\rho)$ is the pdf of the instantaneous SNR, ρ_κ, given in (60). Observe that ρ_κ is a nontrivial function of the κ strongest eigenvalues of the channel matrix $\mathbf{H}^\dagger\mathbf{H}$. Thus, a closed-form expression for the marginal pdf $f_{\rho_\kappa}(\rho)$ and by extension for the average BER in (62) is extremely difficult to obtain. However, we can derive easily computable average BER bounds based only on the marginal cdf of the κ^{th} largest channel eigenvalue given in Lemma 3.1 as done in the following theorem.

Theorem 4.1: The average BER attained by the minimum BER linear transceiver with fixed and equal constellations (assuming κ data symbols per channel use) for the channel models in Definitions 3.1–3.3 can be bounded as

$$\overline{\mathsf{BER}}_\kappa^{(\mathrm{lb})}(\mathsf{snr}) \le \overline{\mathsf{BER}}_\kappa(\mathsf{snr}) \le \overline{\mathsf{BER}}_\kappa^{(\mathrm{ub})}(\mathsf{snr}) \tag{63}$$

with

$$\overline{\mathsf{BER}}_\kappa^{(\mathrm{ub})}(\mathsf{snr}) = \frac{\alpha_\kappa}{2\log_2 M_\kappa}\sqrt{\frac{\beta_\kappa\mathsf{snr}}{2\pi}} \int_0^\infty \frac{e^{-\beta_\kappa\lambda\mathsf{snr}/2}}{\sqrt{\lambda}}F_{\lambda_\kappa}(\lambda)\,d\lambda \tag{64}$$

$$\overline{\mathsf{BER}}_\kappa^{(\mathrm{lb})}(\mathsf{snr}) = \frac{\alpha_\kappa}{2\log_2 M_\kappa}\frac{\beta_\kappa\mathsf{snr}}{\sqrt{2\pi}} \int_0^\infty \frac{e^{-\beta_\kappa(\lambda\mathsf{snr}+\kappa-1)/2}}{\sqrt{\beta_\kappa(\lambda\mathsf{snr}+\kappa-1)}}F_{\lambda_\kappa}(\lambda)\,d\lambda \tag{65}$$

where $F_{\lambda_\kappa}(\cdot)$ is the marginal cdf of the κ^{th} largest eigenvalue given in Lemma 3.1 and the values of the parameters characterizing each channel model given in Tables I and II.

Proof: See Appendix C-I.

Remark 4.1: Observe that $\overline{\mathsf{BER}}_\kappa^{(\mathrm{ub})}(\mathsf{snr})$ in (64) can be used to obtain the exact average BER performance of the channel eigenmodes under the MIMO channel models in Definitions 3.1–3.3 when the power is uniformly distributed among the κ established substreams (see [22] for details).

Remark 4.2: Considering Remark 4.1 and following [22, Theorem 5], the average BER of the minBER-fixed design can be tighter upper-bounded in the high-SNR regime by dividing $\overline{\mathsf{BER}}_\kappa^{(\mathrm{ub})}(\mathsf{snr})$ by κ.

Although Theorem 4.1 provides a numerical procedure to bound the average BER performance of the minBER-fixed design without resorting to the time-comsuming Monte Carlo simulations, it is still difficult to extract any conclusion on how to improve the system performance. Thus, we focus now on the high-SNR regime and provide a simpler performance characterization in terms of the array gain and the diversity gain. Recently, the average BER versus SNR curves of the channel eigenmodes have been parameterized for an uncorrelated Rayleigh channel in [22], [35], and for an uncorrelated Rician channel in [36]. In addition, the performance characterization of the channel eigenmodes has been applied in [22] to analyze the high-SNR global average BER performance of practical linear MIMO transceivers (including the minBER-fixed scheme) in an uncorrelated Rayleigh channel. Using Theorem 3.2, the results in [22] can be straightforwardly extended to include the channel models in Definitions 3.1–3.3 as we present partially in the following theorem.

Theorem 4.2 ([22, Prop. 3])*:* The average BER attained by the minimum BER linear transceiver with fixed and equal constellations (assuming κ data symbols per channel use) for the channel models in Definitions 3.1–3.3 satisfies

$$\overline{\mathsf{BER}}_\kappa(\mathsf{snr}) = (G_{\mathrm{a},\kappa}\cdot\mathsf{snr})^{-G_{\mathrm{d},\kappa}} + o\left(\mathsf{snr}^{-G_{\mathrm{d},\kappa}}\right) \tag{66}$$

where the diversity gain is given by

$$G_{\mathrm{d},\kappa} = (n_\mathsf{T}-\kappa+1)(n_\mathsf{R}-\kappa+1) \tag{67}$$

and the array gain can be bounded as[9]

$$G_{\mathrm{a},\kappa}^{(\mathrm{lb})} \leq G_{\mathrm{a},\kappa} \leq G_{\mathrm{a},\kappa}^{(\mathrm{ub})} \tag{68}$$

with

$$G_{\mathrm{a},\kappa}^{(\mathrm{lb})} = \frac{\beta_\kappa}{\kappa}\left(\frac{\alpha_\kappa}{\log_2 M_\kappa}\frac{a_\kappa 2^{d_\kappa}\Gamma\left(d_\kappa+\frac{3}{2}\right)}{\sqrt{\pi}\kappa(d_\kappa+1)}\right)^{-1/(d_\kappa+1)} \tag{69}$$

$$G_{\mathrm{a},\kappa}^{(\mathrm{ub})} = \kappa\beta_\kappa\left(\frac{\alpha_\kappa}{\log_2 M_\kappa}\frac{a_\kappa I(d_\kappa,\beta_\kappa(\kappa-1))}{\sqrt{2\pi}(d_\kappa+1)}\right)^{-1/(d_\kappa+1)} \tag{70}$$

where $\Gamma(\cdot)$ denotes the gamma function [30, eq. (6.1.1)], $I(d,\beta)$ is[10]

$$I(d,\beta) = \int_{\sqrt{\beta}}^{\infty} e^{-x^2/2}\left(x^2-\beta\right)^{(d+1)} dx \tag{71}$$

and the parameters a_κ and d_κ model the pdf of the κ^{th} largest eigenvalue. They can be obtained using Theorem 3.2 with the values of the parameters for each channel model given in Tables I and II.

In Figs. 2(a) and 3(a), we show the average BER performance of the minBER-fixed design and the average BER bounds derived in Theorem 4.1 in an uncorrelated and a semicorrelated Rayleigh MIMO channel, respectively. In both cases we consider the minBER-fixed scheme with $n_\mathsf{T} = n_\mathsf{R} = 4$, a target transmission rate of $\mathsf{R} = 8$ bits per channel use, and $\kappa = \{2, 4\}$. In Figs. 2(a) and 3(a), we show the high-SNR performance and the parameterized upper and lower average BER bounds (dashed lines) corresponding, respectively, to the lower and upper array gain bounds derived in Theorem 4.2. We only include the beamforming strategy ($\kappa = 1$) in the high-SNR plots, as for this case the upper and lower bounds coincide with the exact average BER. It turns out that for $\kappa > 1$ the proposed average BER upper bound is more convenient to approximate the low SNR performance while the average BER lower bound is very tight in the high-SNR regime.

Finally, it is important to note that the diversity gain given in Theorem 4.2 coincides with the diversity gain achieved with the classical SVD transmission scheme without the additional rotation $\mathbf{Q}_\kappa$ in (56) [22]. Hence, Theorem 4.2 shows that the minBER-fixed design does not provide any diversity advantage with respect to diagonal schemes with simpler channel non-dependent power allocation policies but only a higher array gain. Actually, this statement is not exclusive of the investigated scheme but a common limitation of all linear MIMO transceiver whenever the number of symbols to be transmitted is fixed beforehand (even when using different constellations), as we show in the next theorem.

[9]Observe that an array gain lower bound provides an upper bound on the high-SNR average BER and vice versa.

[10]A closed-form expression for this integral does not exist for a general value of the parameter d; however, it can be easily evaluated for the most common values of d (integers).

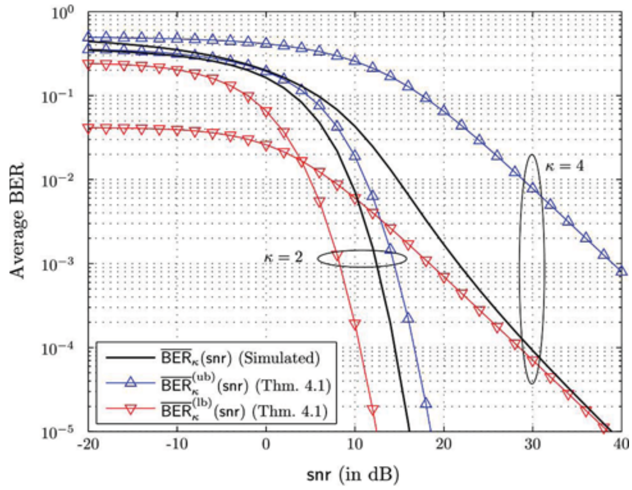

(a) Average BER bounds

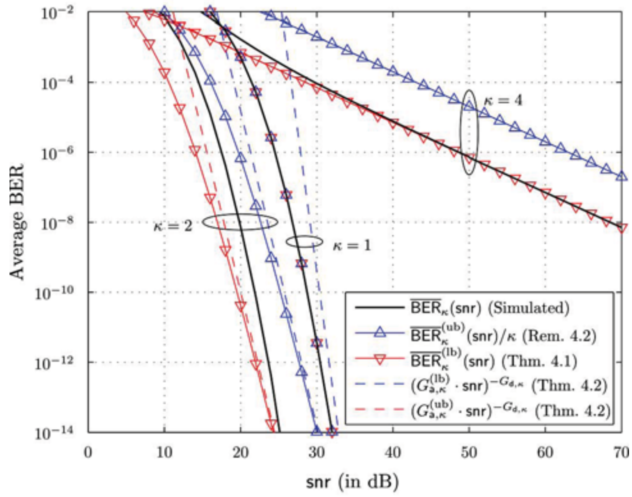

(b) Average BER bounds (high-SNR regime)

Fig. 2. Simulated average BER of the minBER-fixed design and bounds ($n_\mathsf{T} = 4$, $n_\mathsf{R} = 4$, $\kappa = \{1, 2, 4\}$, $\mathsf{R} = 8$) in an uncorrelated Rayleigh fading channel.

Theorem 4.3: The diversity gain attained by any linear MIMO transceiver with fixed constellations (assuming κ data symbols per channel use) for the channel models in Definitions 3.1–3.3 satisfies that

$$G_{\mathrm{d},\kappa} \leq (n_\mathsf{T} - \kappa + 1)(n_\mathsf{R} - \kappa + 1). \tag{72}$$

Proof: The BER averaged over the κ data symbols to be transmitted of any linear MIMO transceiver given in (7) can be lower-bounded as

$$\begin{aligned}\mathsf{BER}_\kappa(\{\rho_{k,\kappa}\}_{k=1}^{\kappa}) &\geq \frac{1}{\kappa}\max_{1\leq k\leq\kappa}\mathsf{BER}_{k,\kappa}(\rho_{k,\kappa})\\ &\geq \frac{1}{\kappa}\min_{\mathbf{A}_\kappa,\mathbf{B}_\kappa}\max_{1\leq k\leq\kappa}\mathsf{BER}_{k,\kappa}(\rho_{k,\kappa}).\end{aligned} \tag{73}$$

The linear MIMO transceiver $(\mathbf{A}_\kappa, \mathbf{B}_\kappa)$ that minimizes the maximum of the BERs as in (73) coincides with the optimum receive and transmit matrices given in (55) and (56), respectively, [14, Sec. 3.4.3.5]. Hence, as the factor $1/\kappa$ does not have any influence on the SNR exponent, the diversity gain of any

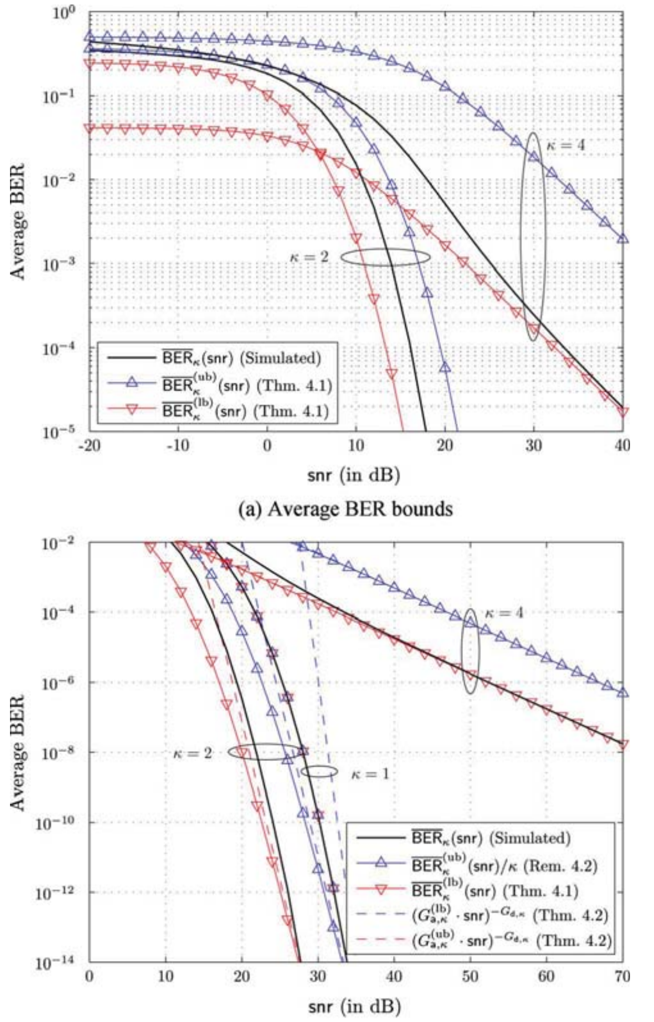

(a) Average BER bounds

(b) Average BER bounds (high-SNR regime)

Fig. 3. Simulated average BER of the minBER-fixed design and bounds ($n_{\mathsf{T}} = 4, n_{\mathsf{R}} = 4, \kappa = \{1, 2, 4\}, \mathsf{R} = 8$) in an semicorrelated Rayleigh fading channel (the correlation matrix is defined as $[\Sigma]_{i,j} = r^{|i-j|}$ with $r = 0.7$).

linear MIMO transceiver is upper-bounded by the one provided in Theorem 4.2. □

Intuitively, the performance of any linear MIMO transceiver is inherently limited by the performance of κ^{th} strongest channel eigenmode, since the design cost function [see, e.g., (11) for the minimum BER design] is evaluated for the κ data symbols to be transmitted, regardless of whether power is allocated to all κ channel eigenmodes during the effective transmission or not. This reveals that the average BER can be improved by introducing the parameter κ into the design criterion, as analyzed in the following section.

V. MinBER Linear MIMO Transceiver With Adaptive Number of Substreams

In this section we derive the minimum BER design with fixed rate and adaptive constellations and analyze analytically its performance.

A. Linear Transceiver Design

The precoding process is here slightly different from classical linear precoding, where the number of data symbols to be transmitted per channel use κ is fixed beforehand. In the following, the parameter κ and the M_κ-dimensional constellations (assumed equal for simplicity) are adapted to the instantaneous channel conditions to minimize the BER by allowing κ to vary between 1 and $n = \min(n_{\mathsf{T}}, n_{\mathsf{R}})$ while keeping the total transmission rate $\mathsf{R} = \kappa \log_2 M_\kappa$ fixed. Usually, only a subset $\mathcal{K}$ of all n possible values of κ is supported, since the number of bits per symbol R/κ has to be an integer. This simple optimization of κ suffices to exploit the full diversity of the channel whenever $\kappa = 1$ is included in $\mathcal{K}$, as will be seen in the next theorem.

Theorem 5.1: The diversity gain attained by any linear MIMO transceiver with adaptive constellations (assuming that the number of data symbols per channel use is chosen optimally from the set $\{1\} \subseteq \mathcal{K} \subseteq \{1, \ldots, n\}$) for the channel models in Definitions 3.1–3.3 satisfies

$$G_{\mathrm{d},\mathcal{K}} = n_{\mathsf{T}} n_{\mathsf{R}} \tag{74}$$

provided that the linear transceiver design reduces to the optimum beamforming scheme for $\kappa = 1$.

Proof: The average BER of any linear MIMO transceiver when κ is optimized to minimize the BER can be upper-bounded using Jensen's inequality [37, Sec. 12.411] as

$$\begin{aligned}\overline{\mathsf{BER}}_{\mathcal{K}}(\mathsf{snr}) &= \mathbb{E}\Big\{ \min_{\kappa \in \mathcal{K}} \mathsf{BER}_\kappa(\{\rho_{k,\kappa}\}_{k=1}^{\kappa}) \Big\} \\ &\leq \min_{\kappa \in \mathcal{K}} \mathbb{E}\{\mathsf{BER}_\kappa\{\rho_{k,\kappa}\}_{k=1}^{\kappa}\} \leq \overline{\mathsf{BER}}_1(\mathsf{snr})\end{aligned} \tag{75}$$

where $\overline{\mathsf{BER}}_1(\mathsf{snr})$ denotes the average BER obtained for $\kappa = 1$. If, in this case, the optimum beamforming scheme is selected, it follows that

$$n_{\mathsf{T}} n_{\mathsf{R}} \geq G_{\mathrm{d},\mathcal{K}} \geq G_{\mathrm{d},1} = n_{\mathsf{T}} n_{\mathsf{R}} \tag{76}$$

where we have used Theorem 4.2 for $\kappa = 1$. Hence, the full diversity of the channel is achieved. □

Observe that a more general setup would also adapt the individual modulations without the constraint of equal constellations. However, the proposed minBER-adap scheme achieves already the full diversity of the channel with low complexity. On top of that, not even the minimum BER linear transceiver with fixed and unequal constellations can be optimally obtained in closed form [38], and this dramatically increases the complexity of the system.

The linear transceiver $(\mathbf{A}_\kappa, \mathbf{B}_\kappa)$ and κ are designed to minimize the BER averaged over the data symbols to be transmitted for all supported values of κ

$$\{\kappa, \mathbf{A}_\kappa, \mathbf{B}_\kappa\} = \arg \min_{\kappa \in \mathcal{K}, \mathbf{A}_\kappa, \mathbf{B}_\kappa} \mathsf{BER}_\kappa(\{\rho_{k,\kappa}\}_{k=1}^{\kappa}) \tag{77}$$

where $\mathbf{B}_\kappa$ has to satisfy the power-constraint in (4) and $\mathsf{BER}_\kappa(\{\rho_{k,\kappa}\}_{k=1}^{\kappa})$ is defined in (7). The optimum linear transceiver $(\mathbf{A}_\kappa, \mathbf{B}_\kappa)$ for a fixed κ and equal constellations has been presented and analyzed in Section IV-B. Using the resulting BER expression in (67), the optimum κ should be selected as

$$\kappa = \arg\min_{\kappa\in\mathcal{K}} \frac{\alpha_\kappa}{\log_2 M_\kappa}\mathcal{Q}\left(\sqrt{\beta_\kappa\rho_\kappa}\right) \tag{78}$$

or, neglecting the contribution of $\alpha_\kappa/\log_2 M_\kappa$ (since it is not in the argument of the Gaussian $\mathcal{Q}$-function), as[11]

$$\kappa = \arg\max_{\kappa\in\mathcal{K}} \beta_\kappa\rho_\kappa \tag{79}$$

where ρ_κ is given in (60).

A similar scheme that adapts the number of substreams under a fixed rate constraint has been proposed in [16] in the context of limited feedback linear precoding. Even assuming perfect CSI, the multimode precoder designed in [16] is still suboptimum, since it does not perform the rotation to ensure equal BER on all substreams, the power is uniformly allocated among the established substreams, and parameter κ is suboptimally chosen as

$$\kappa = \arg\max_{\kappa\in\mathcal{K}} \beta_\kappa\frac{\lambda_\kappa}{\kappa}. \tag{80}$$

A different approach to overcome the diversity limitation of classical linear MIMO transceiver has been also recently given in [39], where the precoder is designed to maximize the minimum Euclidean distance between symbols. However, the diversity order is only increased to $(n_\mathsf{T}-\kappa/2+1)(n_\mathsf{R}-\kappa/2+1)$.

In Fig. 4 we compare the performance of the proposed minBER-adap scheme against the multimode precoder of [16] and the optimum minimum BER linear MIMO transceiver of [38] combined with an exhaustive search over all possible combinations of number of substreams and (possibly unequal) modulation orders which satisfy the rate constraint. We have obtained the average BER performance by numerical simulation in an uncorrelated Rayleigh fading channel for (i) $n_\mathsf{T}=n_\mathsf{R}=4$ and (ii) $n_\mathsf{T}=4$, $n_\mathsf{R}=6$, and a target transmission rate of $\mathsf{R}=8$ bits per channel use. For the minBER-adap design and the multimode precoder, the number of substreams has been adapted with $\mathcal{K}=\{1,2,4\}$ and the corresponding constellations {256-QAM, 16-QAM, QPSK}, while for the optimum minimum BER system all feasible combinations of number of substreams $\{1,2,3,4\}$ and modulations {256-QAM, 128-QAM, 64-QAM, 32-QAM, 16-QAM, 8-QAM, QPSK, BPSK} have been taken into account. As expected, the minBER-adap design offers a better BER performance than the multimode precoder but it is still outperformed by the optimum minimum BER linear transceiver. However, this performance improvement over the proposed scheme does not justify in any case the prohibitive increase of complexity in the optimum design, which implies numerical linear transceiver design and exhaustive search over all possible combinations of substreams and modulations.

B. Analytical Performance

The minimum BER linear transceiver with fixed rate and adaptive constellations has the same structure as the minBER-fixed design presented in Section IV-A but the number of symbols to be transmitted κ is optimally adapted to minimize the BER. Analogously to Section IV-B with the minBER-fixed scheme, we analyze in the following theorems the average BER performance of the minBER-adap design.

[11]Numerical simulations do not show appreciable average BER differences between the selection functions in (84) and in (85) in the BER region of practical interest ($\mathsf{BER} \ll 10^{-1}$).

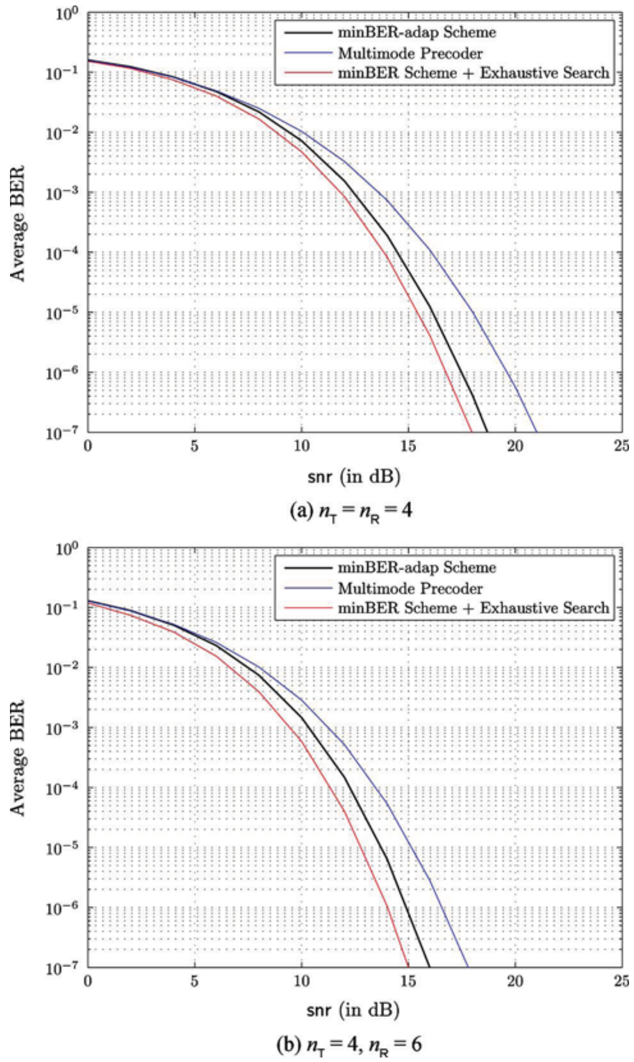

Fig. 4. Simulated average BER of the minBER-adap design ($\kappa=\{1,2,4\}$, $\mathsf{R}=8$), the multimode precoder ($\kappa=\{1,2,4\}$, $\mathsf{R}=8$), and the optimum minimum BER linear transceiver with an exhaustive search over all possible number of substreams and QAM constellations such that $\mathsf{R}=8$ in an uncorrelated Rayleigh fading channel.

Theorem 5.2: The average BER attained by the minimum BER linear transceiver with fixed rate and equal constellations (assuming that the number of data symbols per channel use is chosen from the set $\{1\}\subseteq\mathcal{K}\subseteq\{1,\ldots,n\}$ as in (79)) for the channel models in Definitions 3.1–3.3 can be bounded as

$$\overline{\mathsf{BER}}_\mathcal{K}^{(\mathrm{lb})}(\mathsf{snr}) \le \overline{\mathsf{BER}}_\mathcal{K}(\mathsf{snr}) \le \overline{\mathsf{BER}}_\mathcal{K}^{(\mathrm{ub})}(\mathsf{snr}) \tag{81}$$

with

$$\overline{\mathsf{BER}}_\mathcal{K}^{(\mathrm{ub})}(\mathsf{snr}) = \min_{\kappa\in\mathcal{K}}\left(\frac{\alpha_\kappa}{2\log_2 M_\kappa}\right)\sqrt{\frac{\mathsf{snr}}{2\pi}} \int_0^\infty \frac{e^{-\lambda\mathsf{snr}/2}}{\sqrt{\lambda}} F_{\lambda_\mathcal{K}^{(\mathrm{ub})}}(\lambda)d\lambda \tag{82}$$

$$\overline{\mathsf{BER}}_{\mathcal{K}}^{(\mathrm{lb})}(\mathsf{snr}) = \max_{\kappa\in\mathcal{K}}\left(\frac{\alpha_\kappa}{2\log_2 M_\kappa}\right)\frac{\mathsf{snr}}{\sqrt{2\pi}} \int_0^\infty \frac{e^{-\lambda\mathsf{snr}+\beta_{\mathcal{K}}/2}}{\sqrt{\lambda\mathsf{snr}+\beta_{\mathcal{K}}}} F_{\lambda_{\mathcal{K}}^{(\mathrm{lb})}}(\lambda)d\lambda \quad (83)$$

where $\beta_{\mathcal{K}} = \max_{\kappa\in\mathcal{K}}(\kappa-1)\beta_\kappa$ and we have defined

$$\lambda_{\mathcal{K}}^{(\mathrm{ub})} = \max_{\kappa\in\mathcal{K}}\left(\frac{\beta_\kappa\lambda_\kappa}{\kappa}\right) \text{ and } \lambda_{\mathcal{K}}^{(\mathrm{lb})} = \max_{\kappa\in\mathcal{K}}(\kappa\beta_\kappa\lambda_\kappa). \quad (84)$$

The corresponding cdfs, $F_{\lambda_{\mathcal{K}}^{(\mathrm{ub})}}(\cdot)$ and $F_{\lambda_{\mathcal{K}}^{(\mathrm{lb})}}(\cdot)$, can be obtained using Theorem 3.1 with the values of the parameters for each channel model given in Tables I and II.

Proof: See Appendix C-II.

Remark 5.1: Observe that $\overline{\mathsf{BER}}_{\mathcal{K}}^{(\mathrm{ub})}(\mathsf{snr})$ in (82) coincides with the exact average BER performance of the multimode precoder of [16] except for the factor $\min_{\kappa\in\mathcal{K}}(\alpha_\kappa/2\log_2 M_\kappa)$ which is an upper bound. The corresponding lower bound can be obtained using (134) in Appendix C-II.

Theorem 5.3: The average BER attained by the minimum BER linear transceiver with fixed rate and equal constellations [assuming that the number of data symbols per channel use is chosen from the set $\{1\} \subseteq \mathcal{K} \subseteq \{1,\ldots,n\}$ as in (79)] for the channel models in Definitions 3.1–3.3 satisfies

$$\overline{\mathsf{BER}}_{\mathcal{K}}(\mathsf{snr}) = (G_{\mathrm{a},\mathcal{K}}\cdot\mathsf{snr})^{-G_{\mathrm{d},\mathcal{K}}} + o\left(\mathsf{snr}^{-G_{\mathrm{d},\mathcal{K}}}\right) \quad (85)$$

where the diversity gain is given by

$$G_{\mathrm{d},\mathcal{K}} = n_{\mathsf{T}}n_{\mathsf{R}} \quad (86)$$

the array gain can be bounded as

$$G_{\mathrm{a},\mathcal{K}}^{(\mathrm{lb})} \le G_{\mathrm{a},\mathcal{K}} \le G_{\mathrm{a},\mathcal{K}}^{(\mathrm{ub})} \quad (87)$$

with

$$G_{\mathrm{a},\mathcal{K}}^{(\mathrm{ub})} = \left(\max_{\kappa\in\mathcal{K}}\left(\frac{\alpha_\kappa}{\kappa\log_2 M_\kappa}\right)\frac{a_{\mathcal{K}}^{(\mathrm{ub})}2^{d_{\mathcal{K}}}}{\sqrt{\pi}(d_{\mathcal{K}}+1)}\right)^{-1/(d_{\mathcal{K},\mathrm{u}}+1)} \quad (88)$$

$$G_{\mathrm{a},\mathcal{K}}^{(\mathrm{lb})} = \left(\min_{\kappa\in\mathcal{K}}\left(\frac{\alpha_\kappa}{\log_2 M_\kappa}\right)\frac{a_{\mathcal{K}}^{(\mathrm{lb})}I(d_{\mathcal{K}},\beta_{\mathcal{K}})}{\sqrt{2\pi}(d_{\mathcal{K}}+1)}\right)^{-1/(d_{\mathcal{K}}+1)} \quad (89)$$

where $I(d,\beta)$ is defined (77) and $\beta_{\mathcal{K}} = \max_{\kappa\in\mathcal{K}}(\kappa-1)\beta_K$. The parameters $\{a_{\mathcal{K}}^{(\mathrm{ub})}, d_{\mathcal{K}}\}$ and $\{a_{\mathcal{K}}^{(\mathrm{lb})}, d_{\mathcal{K}}\}$ model the pdfs of $\lambda_{\mathcal{K}}^{(\mathrm{ub})}$ and $\lambda_{\mathcal{K}}^{(\mathrm{lb})}$ defined in (84). They can be obtained using Theorem 3.2 with the values of the parameters for each channel model given in Tables I and II.

Proof: The proof follows from using [22, Lem. 1] and [22, Cor. 1] with the bounds derived in the proof of Theorem 5.2. □

Theorem 5.3 shows that the minimum BER linear transceiver with fixed rate and equal constellations effectively exploits the maximum diversity offered by the MIMO channel whenever $\kappa = 1$ is contained in $\mathcal{K}$. In Fig. 5 we show the average BER performance of the minBER-adap design and of the average BER bounds derived in Theorem 5.2 in an uncorrelated and a semicorrelated Rayleigh fading channel (see details in Fig. 3). We have considered the minBER-fixed scheme with $n_{\mathsf{T}} = n_{\mathsf{R}} = 4$, a target transmission rate of $\mathsf{R} = 8$ bits per channel use, and $\mathcal{K} = \{1,2,4\}$. As expected, the proposed design outperforms the classical minBER-fixed linear transceiver in Figs. 2 and 3.

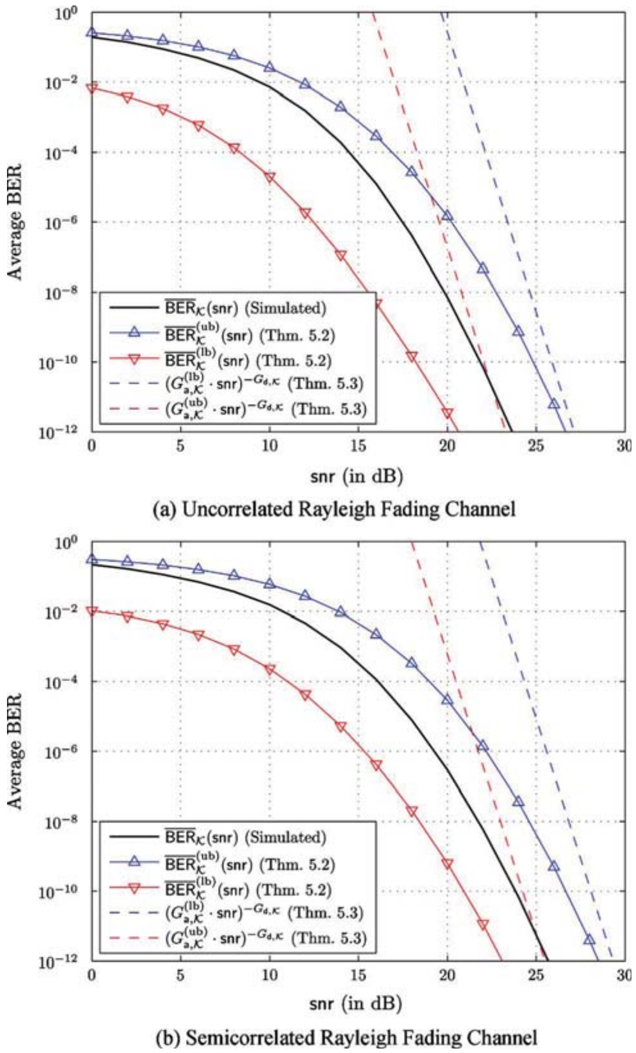

Fig. 5. Simulated average BER of the minBER-adap design and bounds ($n_{\mathsf{T}} = 4, n_{\mathsf{R}} = 4, \mathcal{K} = \{1,2,4\}, \mathsf{R} = 8$).

VI. Conclusion

The contributions of this paper are twofold. The first one relates to linear MIMO system design whereas the second one is more theoretical and provides new probabilistic characterizations of the channel eigenvalues based on the unified formulation of [23]. These results are directly applied to the performance analysis of the investigated schemes.

The linear MIMO transceiver design has been addressed in the literature with the typical underlying assumption that the number of data symbols to be transmitted per channel use is chosen beforehand. In this paper we have proved that, under this assumption, the diversity order of any linear MIMO transceiver is at most driven by that of the weakest channel eigenmode employed, which can be far from the diversity intrinsically provided by the channel. Based on this observation, we have fixed the rate (instead of the number of data symbols) and we have optimized the number of substreams and constellations jointly with the linear precoder. This procedure implies only an additional optimization stage upon the classical design which suffices to extract the full diversity of the channel. Since the ultimate performance of a communication system is given by the BER, we have focused on the minimum BER design. The implications of the proposed optimization have been then illustrated by means of analytical performance analysis of the minimum BER linear MIMO transceiver with fixed and with adaptive number of substreams.

The performance of linear MIMO transceivers is strongly connected to the probabilistic characterization of the ordered eigenvalues of the Wishart, Pseudo-Wishart and Quadratic forms distributions. Based on the general formulation proposed by the same authors in [23], we have derived the cdf of the maximum weighted ordered eigenvalue and the first-order Taylor expansion of both the cdf of the k^{th} largest eigenvalue and the cdf of the maximum weighted ordered eigenvalue for a general class of Hermitian random matrices. This completes the theoretical results presented in [23] and provides the essential mathematical resources needed to investigate the analytical performance of linear MIMO transceivers for typical channel models under a unified framework. In this paper, we have used these results to bound the average BER performance of the investigated minimum BER designs, but they can be similarly applied to other linear transceivers following the procedure in [22]. Additionally, the high-SNR average BER characterization of [22] can be now extended to include other channel models such as the semicorrelated Rayleigh fading and the uncorrelated Rician fading channel.

APPENDIX A
OPERATOR $\mathcal{T}\{\cdot\}$

Definition A.1: The operator $\mathcal{T}\{\cdot\}$ over a tensor $\mathbf{T}$ $(n \times n \times n)$ is defined as[12]

$$\mathcal{T}\{\mathbf{T}\} = \sum_{\boldsymbol{\mu},\boldsymbol{\nu}} \mathrm{sgn}(\boldsymbol{\mu})\mathrm{sgn}(\boldsymbol{\nu}) \prod_{k=1}^{n} [\mathbf{T}]_{\mu_k,\nu_k,k} \tag{90}$$

where the summation over $\boldsymbol{\nu} = (\nu_1, \ldots, \nu_n)$ and $\boldsymbol{\mu} = (\mu_1, \ldots, \mu_n)$ is for all permutations of the integers $(1, \ldots, n)$ and $\mathrm{sgn}(\cdot)$ denotes the sign of the permutation.

Remark A.1: The operator $\mathcal{T}\{\cdot\}$ introduced in Definition A.1 can be alternatively expressed as

$$\mathcal{T}\{\mathbf{T}\} = \sum_{\boldsymbol{\mu},\boldsymbol{\nu}} \mathrm{sgn}(\boldsymbol{\nu}) \prod_{k=1}^{n} [\mathbf{T}]_{\nu_k,k,\mu_k} = \sum_{\boldsymbol{\mu}} |\mathbf{A}(\boldsymbol{\mu})| \tag{91}$$

where matrix $\mathbf{A}(\boldsymbol{\mu})$ $(n \times n)$ is defined as

$$[\mathbf{A}(\boldsymbol{\mu})]_{i,j} = [\mathbf{T}]_{i,j,\mu_j} \quad \text{for } i,j = 1, \ldots, n. \tag{92}$$

[12]Note that this operator was also introduced in [40, Def. 1].

APPENDIX B
ORDERED EIGENVALUES. PROOFS

1. *Proof of Theorem 3.1*

Proof: The cdf of the random variable $\lambda_{\mathcal{K}}$ defined in (21) can be obtained as

$$\begin{aligned} F_{\lambda_{\mathcal{K}}}(\eta) &= \mathsf{Pr}\left(\max_{k\in\mathcal{K}} \left(\frac{\lambda_k}{\theta_k}\right) \le \eta\right) \\ &= \mathsf{Pr}\left(\lambda_{\mathcal{K}_1} \le \theta_1\eta, \ldots, \lambda_{\mathcal{K}_{|\mathcal{K}|}} \le \theta_{\mathcal{K}_{|\mathcal{K}|}}\eta\right) \end{aligned} \tag{93}$$

where $\mathcal{K}_i$ denotes the i^{th} element and $|\mathcal{K}|$ the cardinality of the set $\mathcal{K}$. Defining

$$\tilde{\vartheta}_k(\eta) = \begin{cases} \theta_k\eta & k \in \mathcal{K} \\ \infty & \text{otherwise} \end{cases} \quad \text{for } k = 1, \ldots, n \tag{94}$$

we can rewrite the cdf in (93) as

$$\begin{aligned} F_{\lambda_{\mathcal{K}}}(\eta) &= \mathsf{Pr}\left(\lambda_1 \le \tilde{\vartheta}_1(\eta), \ldots, \lambda_n \le \tilde{\vartheta}_n(\eta)\right) \\ &= F_{\boldsymbol{\lambda}}\left(\tilde{\vartheta}_1(\eta), \ldots, \tilde{\vartheta}_n(\eta)\right) \end{aligned} \tag{95}$$

where $F_{\boldsymbol{\lambda}}(\cdot)$ denotes the joint cdf of the ordered eigenvalues $\lambda_1 \ge \cdots \ge \lambda_n$. Precisely, due to the order of the eigenvalues, for $\eta_{k-1} < \eta_k$ it holds that $F_{\boldsymbol{\lambda}}(\eta_1, \ldots, \eta_{k-1}, \eta_k, \ldots, \eta_n) = F_{\boldsymbol{\lambda}}(\eta_1, \ldots, \eta_{k-1}, \eta_{k-1}, \ldots, \eta_n)$ and, hence, we have that

$$F_{\lambda_{\mathcal{K}}}(\eta) = F_{\boldsymbol{\lambda}}\left(\vartheta_1(\eta), \ldots, \vartheta_n(\eta)\right) \tag{96}$$

where $\vartheta_k(\eta)$ is defined in (23). Finally, the expression of $F_{\lambda_{\mathcal{K}}}(\eta)$ given in the theorem follows from substituting in (96) the joint cdf of the ordered eigenvalues derived in [23, Thm. 3.1]. □

2. *Proof of Theorem 3.2*

Proof: The first-order Taylor expansion of $F_{\lambda_k}(\eta)$ is given by

$$F_{\lambda_k}(\eta) = \left(\frac{F_{\lambda_k}^{(r)}(\eta)|_{\eta=0}}{r!}\right)\eta^r + o(\eta^r) \tag{97}$$

where $F_{\lambda_k}^{(r)}(\eta)$ denotes the r^{th} derivative of $F_{\lambda_k}(\eta)$ (see Lemma 3.1) and r is the smallest integer such that $F_{\lambda_k}^{(r)}(\eta)|_{\eta=0} \ne 0$. Using [41], (10), for the r^{th} derivative of a determinant, $F_{\lambda_k}^{(r)}(\eta)$ can be expressed as

$$F_{\lambda_k}^{(r)}(\eta) = K_{n,m} \sum_{i=1}^{k} \sum_{\boldsymbol{\mu}\in\mathcal{P}(i)} \sum_{\mathbf{r}} \frac{r!}{r_1! \cdots r_n!} |\mathbf{F}^{(\mathbf{r})}(\boldsymbol{\mu}, i; \eta)| \tag{98}$$

where the summation over $\mathbf{r} = (r_1, \ldots, r_n)$ is for all $\mathbf{r}$ such that $r_s \in \mathbb{N} \cup \{0\}$ and $\sum_{s=1}^{n} r_s = r$, and the $n \times n$ matrix $\mathbf{F}^{(\mathbf{r})}(\boldsymbol{\mu}, i; \eta)$ is defined as [see (20)]

$$\begin{aligned} [\mathbf{F}^{(\mathbf{r})}(\boldsymbol{\mu}, i; \eta)]_{u,\mu_v} &= \frac{d^{r_{\mu_v}}}{d\eta^{r_{\mu_v}}} [\mathbf{F}(\boldsymbol{\mu}, i; \eta)]_{u,\mu_v} \\ &= \begin{cases} \frac{d^{r_{\mu_v}}}{d\eta^{r_{\mu_v}}} \int_{\eta}^{\infty} \xi_{u,\mu_v}(\lambda) d\lambda & 1 \le v < i \\ \frac{d^{r_{\mu_v}}}{d\eta^{r_{\mu_v}}} \int_{0}^{\eta} \xi_{u,\mu_v}(\lambda) d\lambda & i \le v \le n \end{cases} \end{aligned} \tag{99}$$

for $u, v = 1, \ldots, n$.Then, the proof reduces to find the minimum integer r such that $F_{\lambda_k}^{(r)}(\eta)$ in (104) does not equal 0 when evaluated at $\eta = 0$. First we determine, for a fixed i and a fixed permutation $\boldsymbol{\mu}$, the set $\{r_{\mu_v}\}_{v=1,\ldots,n}$ with minimum $r(\boldsymbol{\mu}, i) = \sum_{v=1}^{n} r_{\mu_v}$ such that $|\mathbf{F}^{(\boldsymbol{\iota},\mathbf{r})}(\boldsymbol{\mu}, i; \eta = 0)| \neq 0$ and, then, we obtain r as

$$r = \min_{1 \le i \le k} \min_{\boldsymbol{\mu} \in \mathcal{P}(i)} r(\boldsymbol{\mu}, i). \tag{100}$$

Recall from Assumption 3.2 that the Taylor expansion of $\zeta_u(\lambda)\varphi(\lambda)$ is given by

$$\zeta_u(\lambda)\varphi(\lambda) = \sum_{t=c(u)}^{\infty} \frac{a_u(t)}{t!}\lambda^t \tag{101}$$

and, since $\xi_{u,v}(\lambda) = \zeta_u(\lambda)\varphi(\lambda)\lambda^{v-1}$, we have that

$$\begin{aligned}\int_{\eta}^{\infty} \xi_{u,v}(\lambda)d\lambda &= \int_{0}^{\infty} \xi_{u,v}(\lambda)d\lambda - \int_{0}^{\eta} \xi_{u,v}(\lambda)d\lambda \\ &= b_{u,v} - \sum_{t=c(u)+v}^{\infty} \frac{a_{u,v}(t)}{t!}\eta^t \\ &= b_{u,v} + o(\eta^0) \end{aligned} \tag{102}$$

$$\begin{aligned}\int_{0}^{\eta} \xi_{u,v}(\lambda)d\lambda &= \sum_{t=c(u)+v}^{\infty} \frac{a_{u,v}(t)}{t!}\eta^t \\ &= \frac{a_{u,v}(c(u)+v)}{(c(u)+v)!}\eta^{c(u)+v} + o(\eta^{c(u)+v}) \end{aligned} \tag{103}$$

where we have defined

$$\begin{aligned} a_{u,v}(t) &= \frac{(t-1)!}{(t-v)!}a_u(t-v) \quad \text{and} \\ b_{u,v} &= \int_{0}^{\infty} \xi_{u,v}(\lambda)d\lambda. \end{aligned} \tag{104}$$

From (102) and (103) we conclude that r_{μ_v}, such that the columns $[\mathbf{F}^{(\mathbf{r})}(\boldsymbol{\mu}, i; \eta = 0)]_{\mu_v}$ do not have all entries equal to 0, satisfies

$$\begin{cases} r_{\mu_v} = 0 \text{ or } r_{\mu_v} \ge c + \mu_v & 1 \le v < i \\ r_{\mu_v} \ge c + \mu_v & i \le v \le n \end{cases} \tag{105}$$

where $c = \min_u c(u)$.

Note that the condition in (105) is only a necessary condition, as we still have to guarantee that all columns of $\mathbf{F}^{(\mathbf{r})}(\boldsymbol{\mu}, i; \eta = 0)$ are linearly independent in order to assure that $|\mathbf{F}^{(\mathbf{r})}(\boldsymbol{\mu}, i; \eta = 0)| \neq 0$. In fact, the condition in (105) is not sufficient, as in the following we show that the set $\{r_{\mu_v}\}_{v=1,\ldots,n}$ with minimum $r(\boldsymbol{\mu}, i)$ and $|\mathbf{F}^{(\mathbf{r})}(\boldsymbol{\mu}, i; \eta = 0)| \neq 0$ is given by

$$r_{\mu_v} = \begin{cases} 0 & 1 \le v < i \\ c + \mu_v + \nu_{v-i+1} - 1 & i \le v \le n \end{cases} \tag{106}$$

where $\boldsymbol{\nu} = (\nu_1, \ldots, \nu_{n-i+1})$ is a permutation of integers $(1, \ldots, \nu_{n-i+1})$.

Let us focus first on the case $1 \le v < i$ with $r_{\mu_v} = 0$, power allocation policies, i.e.,

$$\begin{aligned} [\mathbf{F}^{(\mathbf{r})}(\boldsymbol{\mu}, i; \eta = 0)]_{\mu_v} &= \frac{d^{r_{\mu_v}}}{d\eta^{r_{\mu_v}}} \int_{0}^{\infty} \xi_{u,\mu_v}(\lambda)d\lambda \Bigg|_{\eta=0} \\ &= b_{u,\mu_v} \end{aligned} \tag{107}$$

for $u = 1, \ldots, n$. For the case $i \le v < n$ we have that

$$\begin{aligned} &[\mathbf{F}^{(\mathbf{r})}(\boldsymbol{\mu}, i; \eta = 0)]_{\mu_v} \\ &\quad = \frac{d^{r_{\mu_v}}}{d\eta^{r_{\mu_v}}} \int_{0}^{\infty} \xi_{u,\mu_v}(\lambda)d\lambda \Bigg|_{\eta=0} \\ &\quad = a_{u,\mu_v}(r_{\mu_v}) \frac{(r_{\mu_v}-1)!}{(r_{\mu_v}-\mu_v)!} a_u(r_{\mu_v} - \mu_v) \end{aligned} \tag{108}$$

for $u = 1, \ldots, n$ and this, noting (105), shows that all r_{μ_v} in the set $\{r_{\mu_v}\}_{v=i,\ldots,n}$ have to be different to force these $n-i+1$ columns not to be linearly dependent. Since the set $\{r_{\mu_v}\}_{v=i,\ldots,n}$ with different elements and minimum $r(\boldsymbol{\mu}, i)$ is

$$r_{\mu_v} = c + \mu_v + \nu_{v-n-i+1} - 1 \tag{109}$$

this confirms (106) as long as $|\mathbf{F}^{(\mathbf{r})}(\boldsymbol{\mu}, i; \eta = 0)| \neq 0$ with

$$\begin{aligned} &[\mathbf{F}^{(\mathbf{r})}(\boldsymbol{\mu}, i; \eta = 0)]_{u,\mu_v} \\ &\quad = \begin{cases} b_{u,\mu_v} & 1 \le v < i \\ a_{u,\mu_v}(c + \mu_v + \nu_{v-n-i+1} - 1) & i \le v \le n \end{cases}. \end{aligned} \tag{110}$$

Now observe that $r = \min_{1 \le i \le k} \min_{\boldsymbol{\mu} \in \mathcal{P}(i)} r(\boldsymbol{\mu}, i)$, with r_{μ_v} as given in (106), is obtained for $i = k$ and $\boldsymbol{\mu}$ satisfying

$$\mu_v = \begin{cases} n + v - k + 1 & 1 \le v < k \\ v - k + 1 & k \le v \le n \end{cases} \tag{111}$$

and that, at least in this case, $|\mathbf{F}^{(\mathbf{r})}(\boldsymbol{\mu}, i; \eta = 0)| \neq 0$ by Assumption 3.2. Thus, r is

$$\begin{aligned} r = \sum_{v=1}^{n} r_v &= (c-1)(n-k+1) + 2\sum_{v=1}^{n-k+1} v \\ &= (c+n-k+1)(n-k+1) \end{aligned} \tag{112}$$

where we have used [33, eq. (0.121.1)]. Finally, we can rewrite $F_{\lambda_k}^{(r)}(\eta)|_{\eta=0}$ as

$$F_{\lambda_k}^{(r)}(\eta)\Big|_{\eta=0} = K_{n,m} \sum_{\boldsymbol{\nu}} \frac{r!}{\tau(\boldsymbol{\nu})} |\mathbf{F}(\boldsymbol{\nu})| \tag{113}$$

where

$$\tau(\boldsymbol{\nu}) = \prod_{v=1}^{n-k+1} (c + v + \nu_v - 1)! \tag{114}$$

and the $n \times n$ matrix $\mathbf{F}(\boldsymbol{\nu})$ is defined, using (106) and (110), as shown in (115) at the bottom of the next page, or, equivalently, using (111) and (104), as shown in (116) at the bottom of the next page. Then, we complete the proof by substituting (113) back in (97).

□

3. Proof of Theorem 3.3

Proof: The first-order Taylor expansion of $F_{\lambda_\mathcal{K}}(\eta)$ is given by

$$F_{\lambda_\mathcal{K}}(\eta) = \left(\frac{F^{(r)}_{\lambda_\mathcal{K}}(\eta)|_{\eta=0}}{r!}\right)\eta^r + o(\eta^r) \tag{117}$$

where $F^{(r)}_{\lambda_\mathcal{K}}(\eta)$ denotes the r^{th} derivative of $F_{\lambda_\mathcal{K}}(\eta)$ (see Theorem 3.1) and r is the smallest integer such that $F^{(r)}_{\lambda_\mathcal{K}}(\eta)|_{\eta=0} \neq 0$. Using the alternative expression of operator $\mathcal{T}\{\cdot\}$ in Remark A.1, we can rewrite $F_{\lambda_\mathcal{K}}(\eta)$ in (23) in terms of sum of determinants. Then, using [41], (10), for the r^{th} derivative of a determinant, it follows

$$F^{(r)}_{\lambda_\mathcal{K}}(\eta) = K_{n,m}\sum_{\mathrm{i}\in\mathcal{S}}\frac{1}{\tau(\boldsymbol{i})}\sum_{\boldsymbol{\mu}}\sum_{\mathbf{r}}\frac{r!}{r_1!\cdots r_n!}|\mathbf{F}^{(\mathbf{r})}(\boldsymbol{\mu},\boldsymbol{i};\boldsymbol{\vartheta}(\eta))| \tag{118}$$

where the summation over $\mathbf{r} = (r_1,\ldots,r_n)$ is for all $\mathbf{r}$ such that $r_s \in \mathbb{N}\cup\{0\}$ and $\sum_{s=1}^n r_s = r$, and the $n\times n$ matrix $\mathbf{F}^{(\mathbf{r})}(\boldsymbol{\mu},\boldsymbol{i};\boldsymbol{\vartheta}(\eta))$ is defined as [see (26)]

$$\begin{aligned}[\mathbf{F}^{(\mathbf{r})}(\boldsymbol{\mu},\boldsymbol{i};\boldsymbol{\vartheta}(\eta))]_{u,\mu_v} &= \frac{d^{r_{\mu_v}}}{d\eta^{r_{\mu_v}}}[\mathbf{T}(\boldsymbol{i};\boldsymbol{\vartheta}(\eta))]_{u,\mu_v,v}\\ &= \frac{d^{r_{\mu_v}}}{d\eta^{r_{\mu_v}}}\int_{\vartheta_{i_v+1}\eta}^{\vartheta_{i_v}\eta}\xi_{u,\mu_v}(\lambda)d\lambda\end{aligned} \tag{119}$$

for $u,v = 1,\ldots,n$. Then, the proof reduces to find the minimum integer r such that $F^{(r)}_{\lambda_\mathcal{K}}(\eta)$ in (118) does not equal 0 when evaluated at $\eta = 0$.

Using the Taylor expansion of $\zeta_u(\lambda)\varphi(\lambda)$ in Assumption 3.2 and recalling that $\xi_{u,v}(\lambda) = \zeta_u(\lambda)\varphi(\lambda)\lambda^{v-1}$, it holds that

$$\begin{aligned}\int_{\vartheta_{i_v+1}\eta}^{\vartheta_{i_v}\eta}\xi_{u,\mu_v}(\lambda)d\lambda &= \int_0^{\vartheta_{i_v}\eta}\xi_{u,\mu_v}(\lambda)d\lambda - \int_0^{\vartheta_{i_v+1}\eta}\xi_{u,\mu_v}(\lambda)d\lambda &(120)\\ &= \sum_{t=c(u)+\mu_v}^{\infty}\frac{a_u(t-\mu_v)}{t(t-\mu_v)!}(\vartheta^t_{i_v} - \vartheta^t_{i_v+1})\eta^t. &(121)\end{aligned}$$

From (120) we conclude that r_{μ_v}, such that the columns $[\mathbf{F}^{(\mathbf{r})}(\boldsymbol{\mu},\boldsymbol{i};\boldsymbol{\vartheta}(\eta=0))]_{\mu_v}$ do not have all entries equal to 0, satisfies

$$r_{\mu_v} \geq c + \mu_v \tag{122}$$

where $c = \min_u c(u)$. Observe that the condition in (122) is only a necessary condition, as we still have to guarantee that all columns of $\mathbf{F}^{(\mathbf{r})}(\boldsymbol{\mu},\boldsymbol{i};\boldsymbol{\vartheta}(\eta=0))$ are linearly independent in order to assure that $|\mathbf{F}^{(\mathbf{r})}(\boldsymbol{\mu},\boldsymbol{i};\boldsymbol{\vartheta}(\eta=0))| \neq 0$. In fact, the condition in (122) is not sufficient, since we have that

$$\begin{aligned}[\mathbf{F}^{(\mathbf{r})}(\boldsymbol{\mu},\boldsymbol{i};\boldsymbol{\vartheta}(\eta=0))]_{\mu_v} &= \frac{(r_{\mu_v}-1)!}{(r_{\mu_v}-\mu_v)!}\\ &\quad\times a_u(r_{\mu_v}-\mu_v)\left(\vartheta^{r_{\mu_v}}_{i_v} - \vartheta^{r_{\mu_v}}_{i_v+1}\right)\end{aligned} \tag{123}$$

for $u = 1,\ldots,n$, and this, noting (122), shows that all r_{μ_v} in the set $\{r_{\mu_v}\}_{v=i,\ldots,n}$ have to be different. The set $\{r_{\mu_v}\}_{v=i,\ldots,n}$ with minimum r and different elements is

$$r_{\mu_v} = c + \mu_v + \nu_v - 1 \tag{124}$$

where $\nu = (\nu_1,\ldots,\nu_n)$ is a permutation of integers $(1,\ldots,n)$. In addition, due to Assumption 3.2, this set ensures that $|\mathbf{F}^{(\mathbf{r})}(\boldsymbol{\mu},i;\boldsymbol{\vartheta}(\eta=0))| \neq 0$, at least when $\boldsymbol{\mu} = \boldsymbol{\nu}$. Thus, independently of $\boldsymbol{i}$ and $\boldsymbol{\mu}$, r is

$$r = \sum_{v=1}^n r_{\mu_v} = (c-1)n + (n+1)n = (c+n)n \tag{125}$$

where we have used [33, eq. (0.121.1)]. Finally, we can rewrite $F^{(r)}_{\lambda_\mathcal{K}}(\eta)|_{\eta=0}$ as

$$\begin{aligned}F^{(r)}_{\lambda_\mathcal{K}}(\eta)\Big|_{\eta=0}\\ = K_{n,m}\sum_{\boldsymbol{i}\in\mathcal{S}}\frac{1}{\tau(\boldsymbol{i})}\sum_{\boldsymbol{\mu}}\sum_{\boldsymbol{\nu}}\frac{r!}{\tau(\boldsymbol{\mu},\boldsymbol{\nu})}|\mathbf{F}(\boldsymbol{\mu},\boldsymbol{\nu},\boldsymbol{i};\boldsymbol{\vartheta})|\end{aligned} \tag{126}$$

where

$$\tau(\boldsymbol{\mu},\boldsymbol{\nu}) = \prod_{v=1}^n (c+\mu_v+\nu_v-1)! \tag{127}$$

and the $n\times n$ matrix $\mathbf{F}(\boldsymbol{\mu},\boldsymbol{\nu},\boldsymbol{i};\boldsymbol{\vartheta})$ is defined as

$$\begin{aligned}[\mathbf{F}(\boldsymbol{\mu},\boldsymbol{\nu},\boldsymbol{i};\boldsymbol{\vartheta})]_{u,\mu_v} &= \frac{(c+\mu_v+\nu_v-2)!}{(c+\nu_v-1)!}\\ &\quad\times a_u(c+\nu_v-1)\left(\vartheta^{r_{\mu_v}}_{i_v} - \vartheta^{r_{\mu_v}}_{i_v+1}\right)\end{aligned} \tag{128}$$

$$[\mathbf{F}(\boldsymbol{\nu})]_{u,\mu_v} = \begin{cases} b_{u,\mu_v} & 1\leq v<k\\ a_{u,\mu_v}(c+\mu_v+\nu_{v-k+1}-1) & k\leq v\leq n\end{cases} \quad \text{for } u,v = 1,\ldots,n \tag{115}$$

$$[\mathbf{F}(\boldsymbol{\nu})]_{u,v} = \begin{cases} \frac{(c+v+\nu_v-2)!}{(c+\nu_v-1)!}a_u(c+\nu_v-1) & 1\leq v\leq n-k+1\\ b_{u,v} & n-k+1<v\leq n\end{cases} \quad \text{for } u,v = 1,\ldots,n. \tag{116}$$

for $u, v = 1, \ldots, n$. Finally, using again Remark A.1, it follows

$$F^{(r)}_{\lambda_{\mathcal{K}}}(\eta)\Big|_{\eta=0} = K_{n,m} \sum_{\boldsymbol{i}\in\mathcal{S}} \frac{r!}{\tau(\boldsymbol{i})} \sum_{\boldsymbol{\mu}} \mathcal{T}\{\mathbf{T}(\boldsymbol{\mu}, \boldsymbol{i}; \boldsymbol{\vartheta})\} \quad (129)$$

where the $n \times n \times n$ tensor $\mathbf{T}(\boldsymbol{\mu}, \boldsymbol{i}; \boldsymbol{\vartheta})$ is defined as

$$[\mathbf{T}(\boldsymbol{\mu}, \boldsymbol{i}; \boldsymbol{\vartheta})]_{u,v,t} = \frac{1}{(c + \mu_v + v - 1)(c + v - 1)!} \times a_u(c + v - 1)\left(\vartheta^{r_v}_{i_t} - \vartheta^{r_v}_{i_t+1}\right) \quad (130)$$

for $u, v, t = 1, \ldots, n$. Then, we complete the proof by substituting (129) back in (117).

□

Appendix C
Performance Analysis Proofs

1. Proof of Theorem 4.1

Proof: The instantaneous SNR of the minBER-fixed design in (66) can be bounded as [22, App. VI]

$$\kappa\lambda_\kappa \mathsf{snr} + (\kappa - 1) \geq \rho_\kappa \geq \frac{\lambda_\kappa \mathsf{snr}}{\kappa}. \quad (131)$$

The proof follows then from calculating the average BER attained with the bounds in (131):

$$\overline{\mathsf{BER}}^{(\mathrm{ub})}_\kappa(\mathsf{snr}) = \frac{\alpha_\kappa}{\log_2 M_\kappa} \int_0^\infty \mathcal{Q}\left(\sqrt{\frac{\beta_\kappa \lambda \mathsf{snr}}{\kappa}}\right) f_{\lambda_\kappa}(\lambda)\, d\lambda \quad (132)$$

$$\overline{\mathsf{BER}}^{(\mathrm{lb})}_\kappa(\mathsf{snr}) = \frac{\alpha_\kappa}{\log_2 M_\kappa} \int_0^\infty \mathcal{Q}\left(\sqrt{\beta_\kappa(\kappa\lambda \mathsf{snr} + (\kappa - 1))}\right) f_{\lambda_\kappa}(\lambda)\, d\lambda. \quad (133)$$

Finally, using integration by parts and the expression of the Gaussian $\mathcal{Q}$-function in (10), we can rewrite (132) and (133) in terms of the cdf of the κ^{th} largest eigenvalue, $F_{\lambda_\kappa}(\cdot)$, and this completes the proof. □

2. Proof of Theorem 5.2

Proof: The average BER of the minBER-adap design with κ chosen from $\mathcal{K}$ as in (85) can be bounded as

$$\min_{\kappa\in\mathcal{K}}\left(\frac{\alpha_\kappa}{\log_2 M_\kappa}\right)\widetilde{\mathsf{BER}}_{\mathcal{K}}(\mathsf{snr}) \leq \overline{\mathsf{BER}}_{\mathcal{K}}(\mathsf{snr}) \leq \max_{\kappa\in\mathcal{K}}\left(\frac{\alpha_\kappa}{\log_2 M_\kappa}\right)\widetilde{\mathsf{BER}}_{\mathcal{K}}(\mathsf{snr}) \quad (134)$$

where $\widetilde{\mathsf{BER}}_{\mathcal{K}}(\mathsf{snr})$ is

$$\widetilde{\mathsf{BER}}_{\mathcal{K}}(\mathsf{snr}) = \int_0^\infty \mathcal{Q}\left(\sqrt{\rho}\right) f_{\rho_{\mathcal{K}}}(\rho)\,d\rho \quad (135)$$

we have defined $\rho_{\mathcal{K}} = \max_{\kappa\in\mathcal{K}}(\beta_\kappa\rho_\kappa)$, and $f_{\rho_{\mathcal{K}}}(\cdot)$ denotes its pdf. Using the bounds of the instantaneous SNR ρ_κ in (131), it holds that

$$\max_{\kappa\in\mathcal{K}}(\kappa\beta_\kappa\lambda_\kappa)\mathsf{snr} + \max_{\kappa\in\mathcal{K}}\beta_\kappa(\kappa - 1) \geq \max_{\kappa\in\mathcal{K}}(\kappa\beta_\kappa\lambda_\kappa \mathsf{snr} + \beta_\kappa(\kappa - 1)) \geq \rho_{\mathcal{K}} \geq \max_{\kappa\in\mathcal{K}}\left(\frac{\beta_\kappa\lambda_\kappa}{\kappa}\right)\mathsf{snr}. \quad (136)$$

Let us define $\lambda^{(\mathrm{ub})}_{\mathcal{K}} = \max_{\kappa\in\mathcal{K}}(\beta_\kappa\lambda_\kappa/\kappa)$ and $\lambda^{(\mathrm{lb})}_{\mathcal{K}} = \max_{\kappa\in\mathcal{K}}(\kappa\beta_\kappa\lambda_\kappa)$ and denote their pdf by $f_{\lambda^{(\mathrm{ub})}_{\mathcal{K}}}(\cdot)$ and $f_{\lambda^{(\mathrm{lb})}_{\mathcal{K}}}(\cdot)$, respectively. The proof follows then from calculating the average BER attained with the bounds in (136) and combining them with (134)

$$\overline{\mathsf{BER}}^{(\mathrm{ub})}_{\mathcal{K}}(\mathsf{snr}) = \max_{\kappa\in\mathcal{K}}\left(\frac{\alpha_\kappa}{\log_2 M_\kappa}\right) \int_0^\infty \mathcal{Q}\left(\sqrt{\lambda \mathsf{snr}}\right) f_{\lambda^{(\mathrm{ub})}_{\mathcal{K}}}(\lambda)\, d\lambda \quad (137)$$

$$\overline{\mathsf{BER}}^{(\mathrm{lb})}_{\mathcal{K}}(\mathsf{snr}) = \min_{\kappa\in\mathcal{K}}\left(\frac{\alpha_\kappa}{\log_2 M_\kappa}\right) \int_0^\infty \mathcal{Q}\left(\sqrt{\lambda \mathsf{snr} + \beta_{\mathcal{K}}}\right) f_{\lambda^{(\mathrm{lb})}_{\mathcal{K}}}(\lambda)\, d\lambda. \quad (138)$$

Finally, we can rewrite (137) and (138) in terms of the cdfs $F_{\lambda^{(\mathrm{ub})}_{\mathcal{K}}}(\cdot)$ and $F_{\lambda^{(\mathrm{lb})}_{\mathcal{K}}}(\cdot)$, respectively, using again integration by parts as in Appendix C-I. □

References

[1] G. J. Foschini, "Layered space-time architecture for wireless communication in a fading environment when using multi-element antennas," *Bell Labs Tech. J.*, vol. 1, no. 2, pp. 41–59, 1996.

[2] G. Foschini and M. Gans, "On limits of wireless communications in a fading environment when using multiple antennas," *Wireless Pers. Commun.*, vol. 3, no. 5, pp. 311–335, 1998.

[3] I. E. Telatar, "Capacity of multi-antenna Gaussian channel," *Eur. Trans. Telecomm.*, vol. 10, no. 6, pp. 585–595, Nov./Dec. 1999.

[4] K. H. Lee and D. P. Petersen, "Optimal linear coding for vector channels," *IEEE Trans. Commun.*, vol. COM-24, pp. 1283–1290, Dec. 1976.

[5] J. Salz, "Digital transmission over cross-coupled linear channels," *AT&T Tech. J.*, vol. 64, no. 6, pp. 1147–1159, Jul.–Aug. 1985.

[6] J. Yang and S. Roy, "On joint transmitter and receiver optimization for multiple-input multiple-output (MIMO) transmission systems," *IEEE Trans. Commun.*, vol. 42, pp. 3221–3231, Dec. 1994.

[7] A. Scaglione, G. B. Giannakis, and S. Barbarossa, "Redundant filter-bank precoders and equalizers part I: Unification and optimal designs," *IEEE Trans. Signal Process.*, vol. 47, pp. 1988–2006, Jul. 1999.

[8] H. Sampath, P. Stoica, and A. Paulraj, "Generalized linear precoder and decoder design for MIMO channels using the weighted MMSE criterion," *IEEE Trans. Commun.*, vol. 49, pp. 2198–2206, Dec. 2001.

[9] A. Scaglione, P. Stoica, S. Barbarossa, G. B. Giannakis, and H. Sampath, "Optimal designs for space-time linear precoders and decoders," *IEEE Trans. Signal Process.*, vol. 50, pp. 1051–1064, May 2002.

[10] E. N. Onggosanusi, A. M. Sayeed, and B. D. V. Veen, "Efficient signaling schemes for wideband space-time wireless channels using channel state information," *IEEE Trans. Veh. Technol.*, vol. 52, pp. 1–13, Jan. 2003.

[11] Y. Ding, T. N. Davidson, Z.-Q. Luo, and K. M. Wong, "Minimum BER block precoders for zero-forcing equalization," *IEEE Trans. Signal Process.*, vol. 51, pp. 2410–2423, Sep. 2003.

[12] Y. Ding, T. N. Davidson, and K. M. Wong, "On improving the BER performance of rate-adaptive block-by-block transceivers with application to DMT," in *Proc. IEEE Global Telecommun. Conf. (GLOBECOM)*, Dec. 2003.

[13] D. P. Palomar, J. M. Cioffi, and M. A. Lagunas, "Joint Tx-Rx beamforming design for multicarrier MIMO channels: A unified framework for convex optimization," *IEEE Trans. Signal Process.*, vol. 51, pp. 2381–2401, Sep. 2003.

[14] D. P. Palomar and Y. Jiang, *MIMO Transceiver Design via Majorization Theory*. Hanover, MA: Now, 2007.

[15] J. B. Andersen, "Antenna arrays in mobile communications: Gain, diversity, and channel capacity," *IEEE Antennas Propag. Mag.*, vol. 42, no. 2, pp. 12–16, Apr. 2000.

[16] D. J. Love and R. W. Heath, Jr, "Multimode precoding for MIMO wireless systems," *IEEE Trans. Signal Process.*, vol. 53, pp. 3674–3687, Oct. 2005.

[17] S. T. Chung and A. J. Goldsmith, "Degrees of freedom in adaptive modulation: A unified view," *IEEE Trans. Commun.*, vol. 49, pp. 1561–1571, 2001.

[18] S. Catreux, V. Erceg, D. Gesbert, and R. W. Heath, Jr, "Adaptive modulation and MIMO coding for broadband wireless data networks," *IEEE Commun. Mag.*, vol. 40, pp. 108–115, Jun. 2002.

[19] X. Zhang and B. Ottersten, "Power allocation and bit loading for spatial multiplexing in MIMO systems," in *Proc. IEEE Int. Conf. Acoust., Speech, Signal Process. (ICASSP)*, 2003, vol. V, pp. 53–56.

[20] Z. Zhou, B. Vucetic, M. Dohler, and Y. Li, "MIMO systems with adaptive modulation," *IEEE Trans. Veh. Technol.*, vol. 54, pp. 1828–1842, Sep. 2005.

[21] D. P. Palomar and S. Barbarossa, "Designing MIMO communication systems: Constellation choice and linear transceiver design," *IEEE Trans. Signal Process.*, vol. 53, pp. 3804–3818, Oct. 2005.

[22] L. G. Ordóñez, D. P. Palomar, A. Pagès-Zamora, and J. R. Fonollosa, "High SNR analytical performance of spatial multiplexing MIMO systems with CSI," *IEEE Trans. Signal Process.*, vol. 55, pp. 5447–5463, Nov. 2007.

[23] L. G. Ordóñez, D. P. Palomar, and J. R. Fonollosa, "Ordered eigenvalues of a general class of Hermitian random matrices with application to the performance analysis of MIMO systems," *IEEE Trans. Signal Process.*, Aug. 2008.

[24] K. Cho and D. Yoon, "On the general BER expression of one- and two-dimensional amplitude modulations," *IEEE Trans. Commun.*, vol. 50, pp. 1074–1080, Jul. 2002.

[25] J. Lassing, E. G. Ström, E. Agrell, and T. Ottosson, "Computation of the exact bit-error rate of coherent m-ary PSK with gray code bit mapping," *IEEE Trans. Commun.*, vol. 51, pp. 1758–1760, Nov. 2003.

[26] M. K. Simon and M. S. Alouini, *Digital Communication Over Fading Channels, Wiley Series in Telecommunications and Signal Processing*, 2nd ed. New York: Wiley, 2002.

[27] Z. Wang and G. B. Giannakis, "A simple and general parameterization quantifying performance in fading channels," *IEEE Trans. Signal Process.*, vol. 51, pp. 1389–1398, Aug. 2003.

[28] A. Zanella, M. Chiani, and M. Z. Win, "A general framework for the distribution of the eigenvalues of wishart matrices," in *Proc. IEEE Int. Conf. Commun. (ICC)*, May 2008.

[29] R. A. Horn and C. R. Johnson, *Topics in Matrix Analysis*. New York: Cambridge Univ. Press, 1991.

[30] M. Abramowitz and I. A. Stegun, *Handbook of Mathematical Functions, with Formulas, Graphs, and Mathematical Tables*. New York: Dover, 1972.

[31] N. G. Bruijn, *Asymptotic Methods in Analysis*, 3rd ed. New York: Dover, 1981.

[32] A. T. James, "Distributions of matrix variates and latent roots derived from normal samples," *Ann. Math. Statist.*, vol. 35, no. 2, pp. 475–501, Jun. 1964.

[33] I. S. Gradshteyn and I. M. Ryzhik, *Table of Integrals, Series, and Products*. New York: Academic, 1980.

[34] M. K. Simon, "The Nuttall Q function- its relation to the Marcum Q function and its application in digital communication performance evaluation," *IEEE Trans. Commun.*, vol. 50, pp. 1712–1715, Nov. 2002.

[35] L. G. Ordóñez, D. P. Palomar, A. Pagès-Zamora, and J. R. Fonollosa, "Analytical BER performance in spatial multiplexing MIMO systems," in *Proc. IEEE Workshop Signal Process. Advan. Wireless Commun. (SPAWC)*, 2005.

[36] S. Jin, X. Gao, and M. R. McKay, "Ordered eigenvalues of complex noncentral Wishart matrices and performance analysis of SVD MIMO systems," in *Proc. IEEE Int. Symp. Inf. Theory (ISIT)*, 2006, pp. 1564–1568.

[37] I. S. Gradshteyn and I. M. Ryzhik, *Table of Integrals, Series, and Product*. New York: Academic, 2000.

[38] D. P. Palomar, M. Bengtsson, and B. Ottersten, "Minimum BER linear transceivers for MIMO channels via primal decomposition," *IEEE Trans. Signal Process.*, vol. 53, no. 8, pp. 2866–2882, Aug. 2005.

[39] B. Vrigneau, J. Letessier, P. Rostaing, L. Collin, and G. Burel, "Extension of the MIMO precoder based on the minimum Euclidean distance: A cross-form matrix," *Proc. IEEE J-STSP Special Issue: MIMO-Optimized Transmiss. Syst. Delivering Data and Rich Content*, vol. 2, no. 2, pp. 135–146, Apr. 2008.

[40] M. Chiani, M. Z. Win, and A. Zanella, "On the capacity of spatially correlated MIMO Rayleigh-fading channels," *IEEE Trans. Inf. Theory*, vol. 49, no. 10, pp. 2363–2371, Oct. 2003.

[41] J. G. Christiano and J. E. Hall, "On the n-th derivative of the j-th order determinant," *Math. Mag.*, vol. 37, no. 4, pp. 215–217, 1964.

Luis G. Ordóñez (S'04) received the electrical engineering degree from the Telecom Barcelona School, Technical University of Catalonia (UPC), Spain, in 2003.

Since 2004, he has been the recipient of a Spanish Ministry of Education and Science Research Assistantship, Department of Signal Theory and Communications, UPC, where he is currently pursuing the Ph.D. degree. From 2001 to 2004, he participated in the European IST projects I-METRA and NEXWAY. Currently, he is involved in the 6th Framework Programme project SURFACE. His research is devoted to study the performance limits of wireless MIMO systems from the information-theoretic and the communication point-of-view.

Daniel P. Palomar (S'99–M'03–SM'08) received the Electrical Engineering and Ph.D. degrees (both with honors) from the Technical University of Catalonia (UPC), Barcelona, Spain, in 1998 and 2003, respectively.

Since 2006, he has been an Assistant Professor with the Department of Electronic and Computer Engineering, Hong Kong University of Science and Technology (HKUST). He has held several research appointments, namely, at King's College London (KCL), London, U.K.; UPC; Stanford University, Stanford, CA; Telecommunications Technological Center of Catalonia (CTTC), Barcelona; Royal Institute of Technology (KTH), Stockholm, Sweden; University of Rome "La Sapienza", Rome, Italy; and Princeton University, Princeton, NJ.

Dr. Palomar is an Associate Editor of the IEEE TRANSACTIONS ON SIGNAL PROCESSING, a Guest Editor of the IEEE *Signal Processing Magazine* 2010 Special Issue on "Convex Optimization for Signal Processing," was a Guest Editor of the IEEE JOURNAL ON SELECTED AREAS IN COMMUNICATIONS 2008 Special Issue on "Game Theory in Communication Systems," as well as the Lead Guest Editor of the IEEE JOURNAL ON SELECTED AREAS IN COMMUNICATIONS 2007 Special Issue on "Optimization of MIMO Transceivers for Realistic Communication Networks." He serves on the IEEE Signal Processing Society Technical Committee on Signal Processing for Communications (SPCOM). He received a 2004/2006 Fulbright Research Fellowship; the 2004 Young Author Best Paper Award by the IEEE Signal Processing Society; the 2002/2003 best Ph.D. prize in Information Technologies and Communications by the UPC; the 2002/2003 Rosina Ribalta first prize for the Best Doctoral Thesis in Information Technologies and Communications by the Epson Foundation; and the 2004 prize for the best Doctoral Thesis in Advanced Mobile Communications by the Vodafone Foundation and COIT.

Alba Pagès-Zamora (S'91–M'03) received the M.S. degree in 1992 and the Ph.D. degree in 1996, both in electrical engineering, from the Universitat Politècnica de Catalunya (UPC), Barcelona, Spain.

In 1992, she joined the Department of Signal Theory and Communications, UPC, and became an Associate Professor in 2001. She teaches graduate and undergraduate courses related to communications and signal processing. Her current research interests include MIMO channel wireless communications and communication in wireless sensor networks. She has published one book chapter, four papers in international periodic journals, and about 35 papers in international conferences. Additionally, she has led two R+D projects with the national industry and was the UPC's Technical Leader of the IST I-METRA and the IST NEXWAY projects. She has also been involved in six national scientific projects, two European IST projects, and one R+D project with the European Space Agency. Currently, she is involved in the 6th Framework Programme IST project SURFACE and is the UPC's Technical Leader of the 6th Framework Programme IST project WINSOC devoted to develop Wireless Sensor Networks with Self-Organization Capabilities for Critical and Emergency Applications.

Javier Rodríguez Fonollosa (S'90–M'92–SM'98) received the Ph.D. degree in electrical and computer engineering from Northeastern University, Boston, MA, in 1992.

In 1993, he joined the Department of Signal Theory and Communications, Universitat Politècnica de Catalunya (UPC), Barcelona, Spain, where he became Associate Professor in 1996, Professor in 2003, and Department Head in 2006. In 1995, he lead UPC's participation in the European Commission-funded ACTS Mobile projects TSUNAMI(II) and SUNBEAM that included the analysis of adaptive antennas in 2on and third generation cellular mobile communication systems. In January 2000, he was appointed Technical and Project Coordinator of the IST project METRA dedicated to the introduction of multiantenna terminals in UMTS. This project continued until 2003 under the name of I-METRA looking into more advanced systems and Systems beyond 3G. From January 2006 to December 2008, he coordinated the Sixth Framework Programme IST project SURFACE which evaluated the performance of a generalized air interface with self-configuration capabilities. Since October 2006, he has been Project Coordinator of the 5-year Type C-Consolider project Fundamental bounds in Network Information Theory of the National Research Plan of Spain. Also since December 2008, he has been Project Coordinator of the 5-year Consolider-Ingenio project COMONSENS on Foundations and Methodologies for Future Communication and Sensor Networks. He is the author of more than 100 papers in the area of signal processing and communications. His research interests include many different aspects of statistical signal processing for communications and information theory.

Dr. Rodríguez Fonollosa was Co-Chairman and Organizer of the IEEE Signal Processing/ATHOS Workshop on Higher-Order Statistics, in June 1995 and September 2001, held in Begur, Girona, Spain, and of the IST Mobile Communications Summit 2001 held in Sitges, Barcelona. He was Elected Member of the Signal Processing for Communications (SPCOM) Technical Committee of the IEEE Signal Processing Society in January 1999. Since May 2005, he has been a member of the Editorial Board of the EURASIP *Signal Processing Journal*.